Title: Toll-Like Receptors 2 and 4 Are Potential Therapeutic Targets Against Peritoneal Dialysis-Associated Fibrosis

Authors: Anne-Catherine Raby,* Chantal S. Colmont,* Ann Kift-Morgan,* Jörg Köhl,[†‡] Matthias Eberl,* Donald Fraser,* Nicholas Topley,* and Mario O. Labéta*

Affiliations: *Division of Infection & Immunity and The Wales Kidney Research Unit, School of Medicine, Cardiff University, Cardiff, United Kingdom; [†]Institute for Systemic Inflammation Research, University of Lübeck, Lübeck, Germany; and [‡]Division of Immunobiology, Cincinnati Children's Hospital, Cincinnati, USA.

Running Title: Reducing Peritoneal Fibrosis

Correspondence: Mario O. Labéta or Anne-Catherine Raby, Division of Infection & Immunity, School of Medicine, Cardiff University, Tenovus Building, Heath Park, Cardiff, CF14 4XN, United Kingdom. E-mail: wmdmol@cardiff.ac.uk; phone: +44(0)2920687019; RabyA@cardiff.ac.uk; phone: +44(0)2920687324; fax: +44 (0)29206 87303.

C. S. C. and A. K.-M. contributed equally to this work.

ABSTRACT

Peritoneal dialysis (PD), an essential renal replacement therapy, remains limited by dialysis failure due to peritoneal membrane fibrosis. This is driven by peritoneal inflammation, caused by infections or sterile cellular stress during PD. Given the fundamental role of Toll-like receptors (TLRs) and complement in inflammation, we assessed the potential of peritoneal TLR2, TLR4, C5aR and C5L2 as therapeutic targets against PD-associated fibrosis. TLR2-, TLR4- and C5aR-mediated pro-inflammatory and fibrotic responses to bacteria were consistent with the expression of these receptors in peritoneal macrophages (TLR2/4, C5aR) and mesothelial cells (TLR2, C5aR). *In vivo*, we found a major role for TLR2, to a lesser extent for TLR4, a supplementary role for C5aR and no apparent activity of C5L2 in infection-induced peritoneal fibrosis development. Similarly, TLR2, TLR4 and C5aR differentially contributed to bacteria-induced pro-fibrotic and inflammatory mediator production by peritoneal leukocytes from uremic PD patients *ex vivo*. TLR2, TLR4 and their co-receptor, CD14, were also involved in pro-fibrotic responses of uremic leukocytes to endogenous components present in non-infected patients' PD effluent (PDE). Enhancing TLR-mediated inflammation increased fibrosis *in vivo*, pointing at TLRs as therapeutic targets. Soluble TLR2 (sTLR2), negative modulator of TLRs, was detected in PDE and inhibited PDE-induced TLR2- or TLR4-mediated pro-fibrotic responses. Notably, sTLR2 markedly reduced Gram-positive and Gram-negative bacteria-induced fibrosis *in vivo*, inhibiting pro-inflammatory and fibrotic genes without affecting infection clearance. These findings reveal peritoneal TLR2 and TLR4's influence on PD-associated infection-induced and sterile fibrosis, and describe a therapeutic strategy to reduce fibrosis by targeting TLRs and CD14 with sTLR2.

INTRODUCTION

Peritoneal dialysis (PD) depends on the structural and functional integrity of the peritoneal membrane. A major factor limiting PD remains peritoneal membrane failure, which is directly related to progressive thickening of the sub-mesothelial compact zone, termed fibrosis, resulting in altered solute transport and dialysis failure. This process is driven by peritoneal inflammation, caused by recurrent infections or by ongoing cellular stress and tissue injury induced by the dialysis process (sterile inflammation).[1] The mechanisms linking inflammation with the genesis and regulation of fibrosis remain to be fully elucidated[2, 3] and effective therapies to prevent this PD-associated pathology are still to be developed.

Toll-like receptors (TLRs) are critical to triggering a rapid inflammatory response to clear infections[4]. They are expressed in various cell types, including peritoneal mesothelial cells,[5] and recognise microorganisms and their components as well as host endogenous molecules released following cellular stress (e.g., High Mobility Group Box-1 (HMGB-1); heat shock proteins), or generated as a consequence of matrix degradation during tissue injury (e.g., hyaluronan, fibronectin).[6, 7] TLR triggering leads to the release of pro-inflammatory and fibrotic mediators, e.g. IL-6, TGF-β, TNF-α, IL-8.[3, 8]

The complement system also plays a fundamental role in inflammation. Complement activation leads to generation of C5a, a potent pro-inflammatory peptide with activities including leukocyte chemoattraction and pro-inflammatory cytokine and chemokine induction. C5a induces responses through the C5a receptor (C5aR). A second C5a receptor, C5L2, can inhibit C5aR.[9-11] We and others have demonstrated crosstalk between TLRs and C5aR, by which cell exposure to a combination of TLR ligands and C5a results in synergistically enhanced pro-inflammatory mediator production.[12-15]

Given the serious inflammatory conditions resulting from TLR and/or C5aR over-activation, TLRs and C5a receptors are attractive therapeutic targets for the treatment and/or prevention of inflammation-associated pathologies.[16-19] In this study, we assessed the potential of

peritoneal TLRs, C5aR and C5L2 as therapeutic targets against peritoneal fibrosis development during PD by investigating their influence on pro-inflammatory and fibrotic responses *in vitro*, *ex vivo* and *in vivo*. The study reveals the major influence that TLR2 and TLR4, and to a lesser extent C5aR, exert on infection-associated and sterile peritoneal inflammation and fibrosis development. It demonstrates the therapeutic potential of a TLR targeting strategy to prevent PD-associated fibrosis that is based on the modulatory capacity of the soluble form of TLR2.

RESULTS

Differential expression and response of TLR2, TLR4 and C5aR in human resident peritoneal leukocytes and mesothelial cells

We first examined the expression and response of TLR2, TLR4 – the TLRs recognising the widest range of microbial components involved in PD-associated infections – and C5aR in the main peritoneal cell types involved in the initial response to danger: resident macrophages, lymphocytes and mesothelial cells (Figure 1A). PD effluent (PDE)-isolated resident macrophages showed high levels of TLR2 and C5aR expression and moderate levels of TLR4, whereas mesothelial cells (from greater omentum) and PDE lymphocytes showed very modest levels of TLR2 and C5aR, and undetectable (mesothelial cells) or barely detectable (lymphocytes) levels of TLR4. The TLR co-receptor CD14, which enhances TLR-mediated responses,[20] was strongly expressed in peritoneal macrophages, but barely detectable in lymphocytes and mesothelial cells. The C5aR modulatory receptor, C5L2, was expressed in all the cell types tested at moderate (macrophages and mesothelial cells) or low (lymphocytes) levels.

Consistent with the expression of the corresponding receptors, TLR2, TLR4 and C5aR agonists triggered pro-inflammatory responses in PDE leukocytes, as judged by the release of the polymorphonuclear (PMN) chemoattractant CXCL8/IL-8 induced by Pam_3-Cys-Ser-$(Lys)_4$ (Pam_3Cys, a synthetic bacterial lipopeptide), the Gram-positive bacterium *Staphylococcus epidermidis* (both TLR2 agonists[21, 22]), the Gram-negative bacterial cell-wall component lipopolysaccharide (LPS) and *Escherichia coli* (both TLR4 agonists[23, 24]) as well as by the C5aR ligand, C5a (Figure 1B). The C5a stimulation profile observed here was similar to that shown by peripheral blood mononuclear cells (PBMC),[15] with reduced stimulation as the C5a concentration increases and the negative regulator C5L2 becomes engaged. Leukocyte responses were mainly driven by macrophages (Figure 1B), as expected given their high receptor expression levels compared with lymphocytes (Figure 1A). Mesothelial cells responded to

Pam_3Cys, *S. epidermidis*, *E. coli* and C5a, but not to LPS (Figure 1B). Their lack of LPS-induced response confirmed our previous findings,[5] since human mesothelial cells did not express TLR4 (Figure 1A). However, they responded to *E. coli*, probably at least partly through the TLR2-mediated recognition of bacterial lipopeptides[25] and the expression of TLR5,[5] which recognises flagellin, the protein component of the flagellum found in Gram-negative bacteria.[26]

Synergism between TLRs and C5aR in the pro- and anti-inflammatory and fibrotic responses of peritoneal leukocytes, but not of mesothelial cells

We tested whether crosstalk between TLRs and C5aR operates in peritoneal cells, as is the case in PBMC, resulting in the synergistic enhancement of responses (Supplemental Figure 1 and ref. 15). Co-stimulation of PDE-isolated leukocytes with Pam_3Cys and C5a resulted in a marked enhancement of IL-8 release compared with the estimated additive effect of each ligand (Figure 2A). A much lower, but significant, synergistic effect was observed upon LPS+C5a stimulation (Figure 2A). By contrast, peritoneal mesothelial cells co-stimulated with varying concentrations of Pam_3Cys+C5a, LPS+C5a or *E. coli*+C5a did not show a synergistic response (Figure 2B). Of note and similar to PBMC,[15] the TLR-C5aR crosstalk in peritoneal leukocytes appears to be negatively regulated by C5L2, as blocking C5L2 with a specific mAb substantially increased the synergistic response to Pam_3Cys+C5a (Figure 2C). Together, these findings indicated the existence of a C5L2-regulated pro-inflammatory TLR-C5aR crosstalk in peritoneal leukocytes, but not in mesothelial cells, by which concerted stimulation via TLR2 – or to a lesser extent via TLR4 – and C5aR imparts hypersensitivity to leukocytes to the cognate ligands.

The potential impact of peritoneal leukocyte TLR2-C5aR crosstalk on fibrosis development was evaluated by testing for synergism in the release of pro- and anti-inflammatory and fibrotic mediators (Figure 2D). Pam_3Cys+C5a induced a marked synergistic enhancement in the release of the pro-fibrotic cytokines TGF-β and IL-13[27-29]. By contrast, the release of other pro-fibrotic and pro-inflammatory cytokines i.e., IL-6 and TNF-α, and the anti-inflammatory and anti-fibrotic cytokine IL-10 showed either a very modest enhancement (IL-6, TNF-α) or only an

additive effect (IL-10) (Figure 2D). Matrix metalloproteinases (MMPs), which are involved in both augmenting and attenuating fibrosis,[30] were only slightly affected by the TLR2-C5aR crosstalk (Figure 2D), with a very modest increase upon Pam_3Cys stimulation at low C5a concentrations (MMP-1, MMP-9) and a stronger synergistic enhancement at higher C5a concentration (MMP-1, MMP-3, MMP-9). By contrast, the effect of TLR2-C5aR crosstalk on a negative regulator of MMPs, tissue inhibitor of metalloproteinases-1 (TIMP-1), was marked and at low C5a concentrations (Figure 2D). These data indicated synergism between TLR2 and C5aR in the release of pro- and anti-inflammatory and fibrotic mediators, with a differential effect depending on the mediator.

Contribution of TLR2, TLR4 and C5aR, but not C5L2 to peritoneal fibrosis development in bacteria-induced mouse peritonitis models

We next evaluated the relevance of peritoneal TLR- and C5a receptor-mediated responses to PD-associated bacteria-induced peritoneal fibrosis development *in vivo*. We used our established[3] murine model of recurrent bacteria-induced peritoneal inflammation leading to fibrosis. In this model, the key features of repeated clinical bacterial peritonitis episodes with the eventual development of peritoneal fibrosis typically observed in PD patients are mimicked by the weekly peritoneal injection (4 injections) of a previously defined dose of whole (heat-killed or live) *S. epidermidis* (TLR2 agonist; a main causative pathogen of PD-associated peritonitis) or *E. coli* (TLR4 agonist) (Supplemental Figure 2 and Concise Methods), both reported to trigger complement activation and C5a generation.[31, 32] Four weeks after the fourth infection/inflammatory episode, peritoneal fibrosis is measured in sections of parietal membrane. Repeated intraperitoneal injection of heat-killed *S. epidermidis* in wild-type (WT) mice resulted in substantial peritoneal fibrosis (Figure 3A). Notably, fibrosis was not observed following *S. epidermidis* injection in TLR2-deficient ($TLR2^{-/-}$) mice (Figure 3A). By contrast, $TLR4^{-/-}$ mice injected with *E. coli* showed a partial (~45%) reduction in fibrosis when compared with WT

mice (Figure 3B), consistent with the possibility that, in addition to TLR4, other receptors (e.g. TLR2, TLR5) may be involved in *E. coli*-induced pro-fibrotic responses.

The role of C5aR and C5aR-TLR2 crosstalk in fibrosis development in mice was also investigated. The repeated injection of heat-killed *S. epidermidis* in $C5aR^{-/-}$ mice resulted in moderate (~40%) fibrosis reduction when compared with WT mice (Figure 3C). This contrasted with the dramatic effect of TLR2 deficiency, which completely prevented fibrosis development (Figure 3A). These findings indicated a prominent role of TLR2 in *S. epidermidis*-induced peritoneal fibrosis development. Furthermore, the absence of fibrosis in the *S. epidermidis*-injected $TLR2^{-/-}$ mice suggested that the locally generated C5a may induce fibrosis mainly indirectly, by enhancing TLR2-mediated responses through the C5aR-TLR2 crosstalk. This putative enhancement may explain the ~40% reduction in fibrosis observed in the *S. epidermidis*-injected $C5aR^{-/-}$ mice (Figure 3C). We therefore tested whether C5L2, which controls peritoneal C5aR-TLR2 crosstalk *in vitro* (Figure 2C), also modulates fibrosis development *in vivo.* Fibrosis was comparable between *S. epidermidis*-injected WT and $C5L2^{-/-}$ mice (Figure 3D), suggesting that the TLR2-C5aR crosstalk signal intermediates involved in pro-fibrotic responses are not controlled by C5L2 or, most likely, that C5L2 controls equally both the pro- and anti-fibrotic signalling demonstrated to be positively affected by TLR2-C5aR crosstalk (Figure 2D). Collectively, these findings indicated a major role for TLR2, to a lesser extent for TLR4 and only a supplementary role for C5aR in bacteria-induced peritoneal fibrosis, but no apparent net influence of C5L2.

Differential contribution of TLR2, TLR4 and C5aR to bacteria-induced pro-fibrotic and inflammatory mediator release by peritoneal leukocytes from uremic PD patients

The clinical relevance of the findings described above was evaluated by testing whether the uremic milieu, present in PD patients, has an effect on the observed role of TLR2, TLR4 and C5aR in bacteria-induced peritoneal fibrosis development. To this end, the involvement of these receptors was evaluated in uremic peritoneal leukocytes isolated from non-infected PDE of

patients whose uremic status was confirmed (urea and creatinine levels in PDE and blood). Consistent with the findings obtained by using the mouse peritonitis model (Figure 3), blocking TLR2, TLR4 and C5aR with specific mAbs significantly reduced *S. epidermidis*- and *E. coli*-induced pro-fibrotic (IL-13, TGFβ, IL-6) and inflammatory (IL-6, IL-8) cytokine release by uremic leukocytes. The extent of the blocking effect depended on the individual, the bacterium and the cytokine tested (Figure 4), with TLR2 blockade consistently showing a significant effect on pro-fibrotic cytokine release.

We also analysed fibrosis-related gene expression in uremic leukocytes following bacterial stimulation and TLR2 blockade. An inhibitory effect of TLR2 blockade on the capacity of *S. epidermidis* to induce mRNA coding for a number of fibrosis markers was observed (Table 1). Twenty three of the 84 genes tested were significantly induced ($P \leq 0.05$; fold change ≥ 2) by *S. epidermidis* (full list of genes in Supplemental Table 1). Notably among the transcripts markedly reduced by blocking TLR2, was that coding for Snail, a transcription factor master regulator of epithelial-mesenchymal transition, a process that plays a critical role in fibrosis development[33]. TLR2 blockade also inhibited a number of *Mmps* transcripts. *Tgf-β* transcription was not induced by *S. epidermidis* at the time point tested (Supplemental Table 1). However, the release of this pro-fibrotic cytokine was induced by *S. epidermidis* after 72h, indicating slower transcription kinetics for this cytokine, and TLR2 blockade reduced this effect markedly (Figure 4). Together, these findings obtained using patients' uremic peritoneal leukocytes tested in a uremic milieu, provided proof of concept for the clinical relevance of the differential involvement of peritoneal TLR2, TLR4 and C5aR in pro-fibrotic and inflammatory responses induced by bacteria.

Involvement of TLR2, TLR4, CD14 and C5aR in PD-induced sterile peritoneal inflammation

To further assess the clinical relevance of peritoneal TLRs and C5aR to PD-associated fibrosis, their involvement in PD-induced sterile inflammation was investigated. Uremic peritoneal

leukocytes isolated from non-infected PDE, were cultured overnight with non-infected cell-free PDE in the absence or presence of TLR2-, TLR4- or C5aR-specific blocking mAbs. The PDE used for stimulation also served to maintain uremic conditions throughout the experiment (Figure 5, A and B). PDE from non-infected PD patients induced pro-fibrotic (IL-13, TGFβ, IL-fhyk6) and inflammatory (IL-6, IL-8, TNF-α) responses in the uremic leukocytes (Figure 5, A and B). These responses were reduced by anti-TLR2, -TLR4 or both mAbs to a varying extent depending on the individual and the PDE tested. TLR2 blockade showed however an overall more consistent effect on pro-fibrotic cytokine release. Additional blocking experiments demonstrated that TLR-mediated peritoneal leukocyte responses to PDE were heavily dependent on the TLR co-receptor CD14, irrespective of the TLR (TLR2 or TLR4) involved (Figure 5, A and B). By contrast, blocking C5aR did not, or very modestly, affect leukocyte responses (Figure 5, A and B). Notably, production of IL-6 and TNF-α - pro-inflammatory and fibrotic mediators reported to be important determinants of peritoneal inflammation and peritoneal solute transport in the uninfected state[1]- was mostly not affected by C5aR blocking (Figure 5, A and B). Similarly, the levels of the pro-fibrotic cytokines TGF-β and IL-13 were not, or very modestly affected, depending on the patient, by C5aR blockade (Figure 5A). These findings indicated that while PD may induce complement production and its activation in the uninfected state, as was reported,[34-37] the direct or indirect (via TLR crosstalk) involvement of complement in pro-inflammatory and fibrotic processes in non-infected patients is modest at best, and depends on the patient. In addition, the peritoneal C5a levels in most patients may be extremely low due to dilution in the peritoneum during dialysis, resulting in minimal C5aR activation.

Analysis of fibrosis-related gene expression in uremic leukocytes following non-infected cell-free PDE stimulation and TLR2 blockade further confirmed the involvement of TLR2 in fibrosis processes (Table 2), Only seven of the 84 genes tested were found affected by PDE stimulation at this time point (full list of genes in Supplemental Table 2), with TLR2 blockade markedly inhibiting *Ccl2* (MCP-1), *Egf* and *Mmp13* (Table 2). *Tgf-β* transcription was not

induced by PDE at this time point (Supplemental Table 2). However, TGF-β release was induced by PDE after 72h, indicating slower transcription kinetics for this cytokine, and blocking TLR2 reduced its release markedly (Figure 5A). Collectively, these findings indicated that peritoneal TLR2, TLR4 and their main co-receptor, CD14, drive pro-fibrotic and inflammatory responses not only to microbial components, but also to host endogenous components that may be present in the uremic peritoneum as a consequence of cellular stress or tissue injury induced during PD.[1] Consistent with this possibility, we found HMGB-1 (TLR2/TLR4 ligand[38, 39]) in PDE of non-infected PD patients, confirming a previous finding,[40] and its expression varied between patients (Figure 5C).

Impact of TLR2-mediated inflammation intensity on bacterial infection-induced peritoneal fibrosis development

To evaluate the importance of peritoneal TLR-mediated inflammation intensity in infection-induced fibrosis development, we used a TLR2-derived peptide – peptide 9 – which we demonstrated amplifies TLR2-mediated inflammation by targeting the TLR co-receptor CD14, enhancing its activity.[20] By using the *in vivo* peritoneal fibrosis model described previously, we found that live *S. epidermidis* infection in the presence of peptide 9 substantially increased peritoneal fibrosis, as compared with mice infected with bacteria in the absence of peptide (Figure 6A). The marked increase in fibrosis in the *S. epidermidis*+peptide 9 mice correlated with higher peritoneal inflammation (higher numbers of PMN and monocytes recruited to the peritoneum, Figure 5A inset). Of note, the TLR2-derived control peptide 17 did not affect inflammatory cell recruitment (Figure 6A inset). Consistent with the higher number of recruited phagocytes, peptide 9 accelerated bacterial clearance (Figure 6A inset). Notably, despite the accelerated infection resolution in the presence of the pro-inflammatory peptide, fibrosis was more severe – probably as a consequence of the enhanced inflammation.

To evaluate the importance of intensity of inflammation over number of infections in peritoneal fibrosis development, mice were injected only twice (one/week) with *S. epidermidis* ±

the TLR2-boosting peptide. Fibrosis was not detected following two infection episodes, even in the presence of the pro-inflammatory peptide (Figure 6B). Together, these findings indicated that, in addition to the number of infection episodes, but irrespective of their duration, the intensity of the resulting inflammation seriously impacts on fibrosis development. This pointed at controlling the intensity of the CD14/TLR-mediated inflammation as a therapeutic strategy against peritoneal fibrosis.

Peritoneal expression and inflammation regulatory capacity of the TLR inhibitor soluble TLR2

To test whether the intensity of the TLR-mediated peritoneal inflammation is naturally controlled, we tested for the peritoneal presence of the natural inhibitor of TLRs, soluble TLR2 (sTLR2), which we previously detected in plasma[41] and demonstrated to reduce TLR-mediated inflammation by acting as a decoy receptor and also by interfering with CD14's co-receptor activity.[42] We detected sTLR2 in PDE from non-infected patients, and its level varied between patients (Figure 7A). The source of sTLR2 was mainly the TLR2-expressing macrophages (Figures 7B and 1A), as PDE-isolated macrophages released sTLR2 upon activation, whereas sTLR2 was barely detectable or undetectable in the culture supernatants of peritoneal lymphocytes and mesothelial cells (Figure 7B). sTLR2 concentrations were significantly increased in PDE from patients with ongoing bacterial peritonitis (Figure 7C), and the levels declined over time, as the infection resolved (Figure 7D).

We next evaluated the capacity of endogenous peritoneal sTLR2 to control inflammatory responses. Depleting sTLR2 from cell-free non-infected PDE significantly increased PDE's stimulatory capacity (Figure 7E), suggesting that the pro-inflammatory capacity of endogenous peritoneal TLR ligands is inhibited by peritoneal sTLR2. Of note, inhibition by sTLR2 was observed in PDE activating cells via TLR2 and TLR4 or mostly via TLR4 (shown here PDE#2 stimulating patient E' leukocytes, Figure 5A and B), suggesting that not only the TLR ligand but also the co-receptor CD14 was targeted for modulation. Importantly, supplementing cell-free

PDE from non-infected or infected patients with purified sTLR2 reduced PDE's stimulatory capacity (Figure 7F), suggesting that, in addition to its natural activity, sTLR2 may be of therapeutic value against infection-induced and sterile peritoneal inflammation and fibrosis development in PD.

Reduction of bacterial-induced peritoneal fibrosis by therapeutic administration of soluble TLR2

We next tested the therapeutic potential of sTLR2 against PD-induced fibrosis *in vivo*. Administration of sTLR2 together with the repeated injection of live *S. epidermidis* prevented fibrosis development (Figure 8A). This was accompanied by a marked reduction in the peritoneal levels of the pro-inflammatory mediators KC (murine functional counterpart of human IL-8) and MCP-1, prototypical PMN, and monocyte chemoattractants, respectively (Figure 8B). This in turn resulted in a reduced number of PMN and monocytes recruited to the peritoneum at the peak time of their influx (Figure 8B).

Analysis of fibrosis-related gene transcripts conducted one week after the last injection (day 28, before fibrosis becomes detectable), showed a marked inhibitory effect of sTLR2 on the capacity of *S. epidermidis* to induce mRNA coding for a number of pro-inflammatory mediators and fibrosis markers (Table 3 and Figure 8C; full list of genes in Supplemental Table 3). Twenty one of the 85 genes tested were significantly induced ($P \leq 0.05$; fold change ≥ 2) by *S. epidermidis* at this time point, and sTLR2 reduced this effect in 18 of them. Among the transcripts affected by sTLR2 was *Fasl*. FasL is central to apoptosis, a cell death mechanism that impairs bacterial clearance during PD and induces peritoneal macrophage death, increases peritoneal inflammation and the production of PMN chemoattractants.[43, 44] The negative effect on *Fasl* was prolonged, as it was also observed after 4 weeks following the last infection (day 49, Table 2). sTLR2 administration also inhibited the *S. epidermidis*-induced transcription of signal transducer and activator of transcription-1 (STAT-1) (Table 1), a critical signal intermediate for fibrosis development in this model.[3] Together with STAT-1, IFN-γ was shown to mediate

peritoneal fibrosis,[3] however, sTLR2 did not significantly affect the strong *S. epidermidis*-induced transcription of IFN-γ (Table 3). sTLR2 may nevertheless affect IFN-γ's pro-fibrotic effect indirectly, through its inhibitory effect on STAT-1 – a main signal intermediate downstream of the IFN-γ receptor. sTLR2 also inhibited the *S. epidermidis*-induced transcription of IL-6 (Table 3), a major driver of peritoneal fibrosis.[3] Notably, sTLR2 counteracted the negative effect of *S. epidermidis* on *Mmp-1*, *Mmp*-3 and *Mmp*-9 observed relatively late (day 49, Table 4), and the relatively early (day 28) *S. epidermidis*' positive effect on *Mmp-13* and the MMP inhibitor *Timp-1* (Table 3). sTLR2's effect on *Timp-1* was maintained until day 49 (Table 4). sTLR2 showed an apparent strong positive effect on *Tnf-α* transcription at day 28 (Table 3), however, this effect was not noticeable at day 49, indicating probably a delayed transcription kinetics rather than an increase in transcript level in the presence of sTLR2. Similarly, an effect on transcription kinetics may explain sTLR2's apparent positive effect on *Ccl3*/*Mip-1α* (Table 3). Transcription of the pro-fibrotic cytokine TGF-β was not induced by *S. epidermidis* either at day 28 or 49 (Supplemental Table 3), whereas its receptor was induced by *S. epidermidis* and inhibited by sTLR2 at day 28 (Table 3). However, analysis of TGF-β levels in peritoneal lavages of mice at 3, 6 and 12 h post-infection, showed induction of TGF-β by *S. epidermidis* and a marked reduction following administration of sTLR2+*S. epidermidis* (Figure 8D).

Of note, the reduced inflammation and phagocyte recruitment in the presence of sTLR2 did not affect the capacity of the mice to clear the infection, as no difference in bacterial load (peritoneum and blood) between sTLR2-treated and -non-treated mice was observed (Figure 8E). This is likely due to the fact that reduced PMN recruitment was significant at the peak of their influx (~12h), and by this time the mice had cleared the infection almost completely. In addition, other immune mechanisms (e.g. complement activation) likely contribute to bacterial clearance.

The fibrosis-preventing capacity of sTLR2 extended to fibrosis induced by Gram-negative bacteria. Administration of sTLR2 together with *E. coli* resulted in reduced peritoneal fibrosis (Figure 8F), although moderate (~35%) when compared with that exerted on *S.*

epidermidis-induced fibrosis (Figure. 8A). This reflects the fact that sTLR2 does not operate as a TLR decoy receptor for most Gram-negative bacterial components, but can still reduce Gram-negative bacteria-induced TLR-mediated fibrotic signalling by inhibiting CD14, a co-receptor for most TLRs[42]. Thus, the therapeutic administration of sTLR2 can inhibit peritoneal fibrosis development induced by repeated peritoneal bacterial infections by acting on a number of pro-inflammatory and fibrotic mediators, but critically, without affecting infection resolution.

DISCUSSION

Peritoneal fibrosis, and the concomitant functional alterations in the peritoneal membrane, is a major cause of PD cessation. It is detected, to a variable extent, in approximately 50% and 80% of patients within one and two years on PD, respectively.[45-47] Peritoneal inflammation is a major driver of fibrosis, and treatment options to reduce or prevent it have been suggested.[1] They include: strategies to improve residual renal function to limit the production and activity of inflammatory cytokines; the use of biocompatible PD solutions to reduce peritoneal membrane injury and cellular stress; the use of catheters resistant to bacterial biofilm formation; the use of twin-bags, Y-set systems and antibiotic administration prior to PD catheter insertion to prevent peritoneal infection, and improvement in fluid status to prevent endotoxemia. In addition, strategies to inhibit the pro-fibrotic activity of TGF-β have been evaluated.[48] However, a limited number of intervention studies have not yet been able to define effective strategies to consistently lower the inflammatory burden in these patients.[1] Critically, studies to identify the main peritoneal receptors involved in triggering the initial pro-inflammatory and fibrotic responses, and to develop therapeutic strategies to reduce their activation have not been conducted. Here, we identified peritoneal TLR2 and TLR4 as critical pro-inflammatory and fibrotic receptors and revealed their potential as therapeutic targets against PD-associated fibrosis development. We described a therapeutic strategy that targets TLRs by using a decoy soluble receptor, sTLR2, which also inhibits the activity of the common TLR co-receptor CD14, thus reducing pro-inflammatory and fibrotic responses to different pathogens and endogenous TLR ligands.

The therapeutic potential of targeting TLRs was highlighted by the pivotal role that TLR2 and TLR4 activation showed in microbial- and sterile inflammation-induced pro-fibrotic responses *in vivo* and *ex vivo* in patients' uremic leukocytes, and the conclusive demonstration that the intensity of the TLR-mediated pro-inflammatory responses dictates the severity of peritoneal fibrosis. Thus, an efficient therapy against peritoneal fibrosis should not only treat

recurrent infections, but also reduce the severity of inflammatory episodes. In this regard, the observation that in our *in vivo* model of bacteria-induced fibrosis the transcript levels of many inflammatory and fibrotic mediators remained elevated long after the resolution of the infectious episode (a finding in agreement with previous reports in clinical PD[49, 50]) highlights the need for a therapy capable of maintaining low levels of these mediators, like the one proposed here.

The potential of sTLR2 as an efficient therapy was further demonstrated by its ability to inhibit peritoneal inflammation and fibrosis development in mice without affecting their capacity to clear the infection. This presents a clear advantage over strategies to block TLR activation completely, for example by using antibodies, as these would be predicted to have a detrimental effect on infection clearance. Preclinical studies have however evaluated combining anti-TLR2/TLR4 antibodies with broad spectrum antibiotics to achieve strong anti-inflammatory effects whilst controlling infection.[51, 52] Thus, a comparative evaluation of the sTLR2 strategy and these alternative therapies in PD models of infection/fibrosis will be required. It also remains to be assessed the efficacy of sTLR2 either as a preventive or therapeutic treatment, since in the present *in vivo* study it was administered together with the infecting bacteria. Due to its ability to target both the TLR ligand and the common TLR co-receptor, CD14, sTLR2 presents a dual therapeutic benefit, as demonstrated here by its capacity to inhibit proinflammatory and fibrotic responses in models of Gram-positive as well as Gram-negative bacterial peritoneal infections and in patients' sterile PDE activating cells via TLR2 or TLR4. The sTLR2-based anti-fibrotic strategy described here could thus prove to be a valuable adjunct to standard antibiotic therapies during PD infections or to more biocompatible PD solutions. sTLR2's capacity to modulate CD14 activity would also be potentially useful against fungal and viral infections in which TLRs other than TLR2 and TLR4 are involved. It may also be potentially useful in fibrosis-associated conditions of organs such as the kidney, lung and liver and in other PD-associated inflammatory conditions, for example to help reduce the elevated risk of cardiovascular diseases.[53]

CONCISE METHODS

Cells and PD Effluent

Samples from healthy individuals (omentum, blood) and PD patients (spent PD dialysate) were obtained in accordance with the institutional review board of Cardiff University and the local National Health Service Research Ethics Committee. Written informed consent was obtained from all donors. Sampling was carried out within the UK Clinical Research Network under study portfolios ID #11838 (PERITPD) and ID #11839 (LEUKPD) and adhered to the Declaration of Helsinki. Spent PD dialysates were obtained from continuous ambulatory PD patients following an overnight dwell). Resident peritoneal leukocytes were obtained by centrifugation (2 times, 425 x g x 15 min, 4 °C) of non-infected dialysates and were cultured in RPMI 1640 medium (Invitrogen) supplemented with 10% foetal calf serum (FCS, HyClone; < 0.06 U/mL endotoxin; heat-inactivated, 56 °C, 30 min). The cell-free (centrifuged) dialysate supernatants were aliquoted and kept frozen (-85 °C) until further use. To confirm the uremic status of the patients, the levels of urea and creatinine in the PDE and blood were tested (Cardiff and Vale University Hospital, clinical Pathology laboratory). Uremia was defined as urea > 7.8 mM and creatinine > 110 μM (UK-wide criteria defined by the NHS).

Peritoneal lymphocytes and macrophages were isolated from freshly-prepared PDE-leukocytes following adhesion (2h, 37 °C) in the absence of serum. The purity of the macrophage (adherent fraction, ≥ 90%) and lymphocyte (non-adherent fraction, ≥ 95%) populations was determined by flow cytometry, based on their forward and side scatter properties and CD14 expression levels. Cell viability was assed using the eFluor viability dye (eBioscience) and was always ≥85%.

Peritoneal mesothelial cells were prepared by tryptic digest of omental biopsies obtained following elective surgery of non-PD patients, as previously described,[5] and cultured in M199 medium (Invitrogen) supplemented with insulin (0.5 μg/ml), transferrin (0.5 μg/ml), and 10% FCS.

Human PBMC were obtained through Ficoll density-gradient centrifugation and cultured in RPMI 1640 medium supplemented with 10% FCS.

Functional Assays

For activation experiments (Figures 1, 2 and 4), triplicate aliquots of peritoneal leukocytes, lymphocytes, macrophages and PBMC (1.5 x 10^4 cells/well, in 96-well plates) or mesothelial cells (4 x 10^4 cells/well, in 48 well-plates), were cultured in the presence of the indicated concentrations of ultra-pure LPS (*E. coli* O111:B4 strain; Invivogen), the synthetic bacterial lipopeptide Pam_3-Cys-Ser-$(Lys)_4$ HCl (EMC microcollections), heat-killed *E. coli* (O111:B4 strain; Invivogen) or heat-killed (20 min, 100 °C) *S. epidermidis* (ATCC 12228), in the absence or presence of the indicated concentrations of purified human C5a (Comptech). For the experiments shown in Figure 4, the medium was supplemented with the patients' own PDE (1:2 dilution) in order to maintain the uremic milieu throughout the experiment. Cell culture supernatants were collected for cytokine assays following 16h stimulation. For TGF-β determinations, cells were washed (RPMI 1640) after 48h stimulation and cultured for a further 24h in the absence of FCS before culture supernatants were collected. Supernatants were tested for IL-8, TGF-β, IL-13 and TIMP-1 by ELISA (R&D Systems) and IL-6, TNF-α, IL-10, MMP-1, MMP-3 and MMP-9 by using the multiplex ELISA platform Meso Scale Discovery. RNA was extracted and gene array analyses were performed as described below.

For testing cell responses to sterile cell-free PDE supernatants (Figure 5), peritoneal leukocytes (1.5 x 10^4 cells/well) were stimulated with PDE (1:2 dilution) from patients with no ongoing clinical peritoneal infection and no history of infection in the 6 months prior to PDE collection. The sterility of the cell-free PDE used was confirmed by negative bacterial growth (on microbiological agar plates) and bacterial DNA detection by qPCR. Briefly, total DNA was extracted from cell-free PDE of non-infected patients by a chelex-based method as previously described.[54] One PDE sample was spiked with heat-killed *S. epidermidis* prior to extraction to

serve as a positive control. Pan-bacterial DNA was then amplified by qPCR using the Femto™ Bacterial DNA Quantification kit (Zymo research), and the amount of DNA in PDE was determined using the kit's internal standard curve as a reference. A Ct of 30 cycles, corresponding to 10 fg of bacterial DNA per 1ml of PDE, was set as cut off for PDE sterility (Supplemental Figure 3).

sTLR2 depletion from PDE before cell stimulations was performed as previously described[41] by sequential immunoprecipitations (4 rounds) with the purified polyclonal anti-TLR2 Ab TLR2p (generated in our laboratories[41] by immunization with an N terminus 20-mer TLR2 peptide, SKEESSNGASLSGDRNGIGK) or isotype control (mock depletion; purified rabbit Igs, Sigma). The extent of the sTLR2 depletion was up to 85%, depending on the experiment, as judged by Western blotting followed by densitometric analysis of the gels. In some experiments (Figure 7) sTLR2 levels in PDE were determined by ELISA (R&D Systems). For the experiment shown in Figure 7F, PDE-induced cell stimulation was conducted in the presence of human recombinant soluble TLR2 (500 ng/ml, R&D).

For blocking experiments, cells were preincubated (30 min at 37 °C) with 5 μg/ml of functional grade anti-TLR2 (clone T2.5, eBioscience), anti-TLR4 (clone3C3, Hycult), anti-CD14 (clone MY4, Beckman Coulter) or anti-C5aR (clone S5/1, Hycult) blocking mAbs or the corresponding isotype-matched control.

Flow Cytometry

TLR2, TLR4, CD14 and C5aR cell surface expression was determined by flow cytometry as previously described[55] using anti-TLR2 (clone T2.5), anti-TLR4 (clone 15C1), anti-CD14 (clone MY4) and anti-C5aR (clone S5/1) mAbs and isotype-matched controls. To determine C5L2 expression levels, staining with a PE-conjugated anti-C5L2 specific mAb (clone 1D9, Biolegend) was performed at room temperature, to allow for Ab internalisation and detection of intracellular C5L2. Peritoneal lymphocytes and macrophages were identified in the peritoneal

leukocyte preparations from PDE by their CD14 staining and forward and side scatter profiles (Supplemental Figure 4). Cell viability (eFluor viability dye) was always ≥85%.

In Vivo experiments

All procedures were carried out under a Home Office project license. Inbred 8 to 10-wk-old wild-type (C57/BL6J, C57BL/10J and BALB/cJ), TLR2$^{-/-}$ (B6.129-*Tlr2*^{tm1Kir}/J), TLR4$^{-/-}$ (C57BL/10ScNJ) and C5aR$^{-/-}$ (C.129S4(B6)-*C5ar1*^{tm1Cge}/J) mice were obtained from Jackson laboratories, and C5L2$^{-/-}$ mice (on a BALB/c background) were bred and maintained in J. Köhl's laboratory, Germany. Mice were intraperitoneally inoculated with PBS (500 µl), SES (a *S. epidermidis* cell-free supernatant prepared as previously described[56]), heat-killed or live *S. epidermidis* (5 x 10^8 CFU/mouse) or heat-killed *E. coli* (2 x 10^7 CFU/mouse), in the absence or presence of previously defined optimal doses of the TLR2-derived peptide 9 (TNSLIKKFTFRNVKITDESLFQVMKLLN, 20 µg/mouse, > 95% pure, Lifetein)[20] or human recombinant soluble TLR2[42] (250 ng/mouse). Injections were repeated weekly, for 4 or 2 weeks as indicated, and mice were then left untreated for a week (Day 28) or 4 weeks (Day 49) before parietal peritoneal membrane was collected for fibrosis assessment. Through the use of this model (4 injections, one/week), fibrosis became detectable at day 49 following repeated injection with SES and whole (heat-killed or live) *S. epidermidis* or *E. coli* as well as by injection of PBS, albeit to a much lesser extent (Supplemental Figure 2). The latter most likely resulted from sterile inflammation induced by tissue injury/cellular stress. SES, *S. epidermidis* and *E. coli* are known to induce cell responses mainly via TLR2 (SES,[5] *S. epidermidis*[21]) and TLR4 (*E. coli*[23, 24]).

For determination of leukocyte numbers, cytokine levels and bacterial load, mice were sacrificed at the indicated time points after the first injection, their peritoneal cavity was lavaged with 2 ml of ice-cold PBS, and peripheral blood was obtained by cardiac puncture. Leukocyte numbers in the lavages were determined by Coulter counting (Coulter Z2, Beckman-Coulter) and differential double staining (anti-Ly6-PE, BD; anti-7/4-A647, Serotec) followed by flow cytometric analysis.

Cytokine levels were determined by ELISA, and bacterial CFU in peritoneal lavages and blood samples, by culturing on Mueller-Hinton agar plates (Oxoid) overnight at 37 °C.

Peritoneal Membrane Histology

Peritoneal membrane biopsies were fixed (24h, 4 °C) with a neutral buffered 10% formalin solution (Sigma) saline embedded in paraffin, and sections (5 μm thickness) were stained with hematoxylin and eosin. Slides were analysed with a Leica DFC49 microscope (×40 objective) and camera, and the thickness of the submesothelial cell compact zone (SMC) was measured as previously described.[3] Briefly, three different fields of view were examined for each mouse, 6 measurements were made per field and the average of the 10 highest measurements was taken as mean of SMC thickness for each animal.

Western Blotting

The Western Blot technique was as previously described.[57] Cell-free PDE samples were diluted 1/20 in Laemmli reducing sample buffer and subjected to 10% SDS-PAGE prior to Western blot analysis using the anti-TLR2 polyclonal Ab TLR2p described above (1/2000) or an anti-HMGB1 polyclonal Ab (Ab18256, Abcam, 1/1000). Densitometric analysis was performed using the ImageJ software.

Fibrosis-focused Gene Arrays

Total RNA was isolated from peritoneal leukocytes or mice peritoneal membranes using the RNeasy mini kit (Qiagen). Reverse transcription-polymerase chain reaction (RT-PCR) was performed on 200 ng of RNA using the RT^2 first strand kit (Qiagen, including a genomic DNA elimination step). Fibrosis gene array RT-qPCR was performed on the resulting complementary DNA (cDNA) using the human or mouse fibrosis RT^2 Profiler PCR Array (85 genes; Qiagen) and the ABI ViiA7^{TM} thermocycler. The results were analysed using Qiagen software. Changes in gene expression compared to control were considered statistically significant when $P<0.05$,

and biologically relevant when the fold change was ≤ 0.5 or ≥ 2, as recommended by the manufacturer. The complete data set is shown in Supplemental Table 1.

Statistical Analysis

Statistical analysis of the data was performed by using an unpaired Student's *t* test. *P* values of less than 0.05 were considered significant.

ACKNOWLEDGMENTS

We thank M. López-Cabrera (Centro de Biología Molecular-Severo Ochoa-CSIC, Madrid, Spain), C. Fielding (Cardiff University, UK), and J. E. Rey Nores (Cardiff Metropolitan University, UK) for critical comments and reading of the manuscript.

This work was supported by grants from The National Institute of Social Care and Health Research (NISCHR), Wales (to M.O.L. and M.E.); NISCHR and Kidney Research UK (KRUK) Fellowships (to A.-C.R.); KRUK project grant (to M. E.) and SFB/TR22 of the Deutsche Forschung Germany (J.K.).

DISCLOSURES

None

REFERENCES

1. Cho, Y, Hawley, CM, Johnson, DW: Clinical causes of inflammation in peritoneal dialysis patients. *International journal of nephrology,* 2014**:** 909373, 2014.
2. Lambie, M, Chess, J, Donovan, KL, Kim, YL, Do, JY, Lee, HB, Noh, H, Williams, PF, Williams, AJ, Davison, S, Dorval, M, Summers, A, Williams, JD, Bankart, J, Davies, SJ, Topley, N, Global Fluid Study, I: Independent effects of systemic and peritoneal inflammation on peritoneal dialysis survival. *Journal of the American Society of Nephrology : JASN,* 24**:** 2071-2080, 2013.
3. Fielding, CA, Jones, GW, McLoughlin, RM, McLeod, L, Hammond, VJ, Uceda, J, Williams, AS, Lambie, M, Foster, TL, Liao, CT, Rice, CM, Greenhill, CJ, Colmont, CS, Hams, E, Coles, B, Kift-Morgan, A, Newton, Z, Craig, KJ, Williams, JD, Williams, GT, Davies, SJ, Humphreys, IR, O'Donnell, VB, Taylor, PR, Jenkins, BJ, Topley, N, Jones, SA: Interleukin-6 signaling drives fibrosis in unresolved inflammation. *Immunity,* 40**:** 40-50, 2014.
4. Kawai, T, Akira, S: The role of pattern-recognition receptors in innate immunity: update on Toll-like receptors. *Nat Immunol,* 11**:** 373-384, 2010.
5. Colmont, CS, Raby, AC, Dioszeghy, V, Lebouder, E, Foster, TL, Jones, SA, Labeta, MO, Fielding, CA, Topley, N: Human peritoneal mesothelial cells respond to bacterial ligands through a specific subset of Toll-like receptors. *Nephrology, dialysis, transplantation : official publication of the European Dialysis and Transplant Association - European Renal Association,* 26**:** 4079-4090, 2011.
6. Chen, GY, Nunez, G: Sterile inflammation: sensing and reacting to damage. *Nat Rev Immunol,* 10**:** 826-837, 2010.
7. Anders, HJ, Schaefer, L: Beyond tissue injury-damage-associated molecular patterns, toll-like receptors, and inflammasomes also drive regeneration and fibrosis. *Journal of the American Society of Nephrology : JASN,* 25**:** 1387-1400, 2014.
8. Kawasaki, T, Kawai, T: Toll-like receptor signaling pathways. *Frontiers in immunology,* 5**:** 461, 2014.
9. Rittirsch, D, Flierl, MA, Nadeau, BA, Day, DE, Huber-Lang, M, Mackay, CR, Zetoune, FS, Gerard, NP, Cianflone, K, Kohl, J, Gerard, C, Sarma, JV, Ward, PA: Functional roles for C5a receptors in sepsis. *Nat Med,* 14**:** 551-557, 2008.
10. Chen, NJ, Mirtsos, C, Suh, D, Lu, YC, Lin, WJ, McKerlie, C, Lee, T, Baribault, H, Tian, H, Yeh, WC: C5L2 is critical for the biological activities of the anaphylatoxins C5a and C3a. *Nature,* 446**:** 203-207, 2007.
11. Bamberg, CE, Mackay, CR, Lee, H, Zahra, D, Jackson, J, Lim, YS, Whitfeld, PL, Craig, S, Corsini, E, Lu, B, Gerard, C, Gerard, NP: The C5a receptor (C5aR) C5L2 is a modulator of C5aR-mediated signal transduction. *J Biol Chem,* 285**:** 7633-7644.
12. Riedemann, NC, Guo, RF, Hollmann, TJ, Gao, H, Neff, TA, Reuben, JS, Speyer, CL, Sarma, JV, Wetsel, RA, Zetoune, FS, Ward, PA: Regulatory role of C5a in LPS-induced IL-6 production by neutrophils during sepsis. *Faseb J,* 18**:** 370-372, 2004.
13. Zhang, X, Kimura, Y, Fang, C, Zhou, L, Sfyroera, G, Lambris, JD, Wetsel, RA, Miwa, T, Song, WC: Regulation of Toll-like receptor-mediated inflammatory response by complement in vivo. *Blood,* 110**:** 228-236, 2007.
14. Wang, M, Krauss, JL, Domon, H, Hosur, KB, Liang, S, Magotti, P, Triantafilou, M, Triantafilou, K, Lambris, JD, Hajishengallis, G: Microbial hijacking of complement-toll-like receptor crosstalk. *Sci Signal,* 3**:** ra11.
15. Raby, AC, Holst, B, Davies, J, Colmont, C, Laumonnier, Y, Coles, B, Shah, S, Hall, J, Topley, N, Kohl, J, Morgan, BP, Labeta, MO: TLR activation enhances C5a-induced pro-inflammatory responses by negatively modulating the second C5a receptor, C5L2. *Eur J Immunol,* 41**:** 2741-2752, 2011.
16. Kanzler, H, Barrat, FJ, Hessel, EM, Coffman, RL: Therapeutic targeting of innate immunity with Toll-like receptor agonists and antagonists. *Nat Med,* 13**:** 552-559, 2007.
17. Dunne, A, Marshall, NA, Mills, KH: TLR based therapeutics. *Curr Opin Pharmacol,* 11**:** 404-411, 2011.
18. Mollnes, TE, Christiansen, D, Brekke, OL, Espevik, T: Hypothesis: combined inhibition of complement and CD14 as treatment regimen to attenuate the inflammatory response. *Adv Exp Med Biol,* 632**:** 253-263, 2008.

19. Riedemann, NC, Guo, RF, Ward, PA: Novel strategies for the treatment of sepsis. *Nat Med,* 9**:** 517-524, 2003.
20. Raby, AC, Holst, B, Le Bouder, E, Diaz, C, Ferran, E, Conraux, L, Guillemot, JC, Coles, B, Kift-Morgan, A, Colmont, CS, Szakmany, T, Ferrara, P, Hall, JE, Topley, N, Labeta, MO: Targeting the TLR co-receptor CD14 with TLR2-derived peptides modulates immune responses to pathogens. *Science translational medicine,* 5**:** 185ra164, 2013.
21. Strunk, T, Power Coombs, MR, Currie, AJ, Richmond, P, Golenbock, DT, Stoler-Barak, L, Gallington, LC, Otto, M, Burgner, D, Levy, O: TLR2 mediates recognition of live Staphylococcus epidermidis and clearance of bacteremia. *PloS one,* 5**:** e10111, 2010.
22. Zahringer, U, Lindner, B, Inamura, S, Heine, H, Alexander, C: TLR2 - promiscuous or specific? A critical re-evaluation of a receptor expressing apparent broad specificity. *Immunobiology,* 213**:** 205-224, 2008.
23. Hoshino, K, Takeuchi, O, Kawai, T, Sanjo, H, Ogawa, T, Takeda, Y, Takeda, K, Akira, S: Cutting edge: Toll-like receptor 4 (TLR4)-deficient mice are hyporesponsive to lipopolysaccharide: evidence for TLR4 as the Lps gene product. *J Immunol,* 162**:** 3749-3752, 1999.
24. Roger, T, Froidevaux, C, Le Roy, D, Reymond, MK, Chanson, AL, Mauri, D, Burns, K, Riederer, BM, Akira, S, Calandra, T: Protection from lethal gram-negative bacterial sepsis by targeting Toll-like receptor 4. *Proc Natl Acad Sci U S A,* 106**:** 2348-2352, 2009.
25. Elson, G, Dunn-Siegrist, I, Daubeuf, B, Pugin, J: Contribution of Toll-like receptors to the innate immune response to Gram-negative and Gram-positive bacteria. *Blood,* 109**:** 1574-1583, 2007.
26. Hayashi, F, Smith, KD, Ozinsky, A, Hawn, TR, Yi, EC, Goodlett, DR, Eng, JK, Akira, S, Underhill, DM, Aderem, A: The innate immune response to bacterial flagellin is mediated by Toll-like receptor 5. *Nature,* 410**:** 1099-1103, 2001.
27. Kaviratne, M, Hesse, M, Leusink, M, Cheever, AW, Davies, SJ, McKerrow, JH, Wakefield, LM, Letterio, JJ, Wynn, TA: IL-13 activates a mechanism of tissue fibrosis that is completely TGF-beta independent. *J Immunol,* 173**:** 4020-4029, 2004.
28. Leask, A, Abraham, DJ: TGF-beta signaling and the fibrotic response. *FASEB J,* 18**:** 816-827, 2004.
29. Pohlers, D, Brenmoehl, J, Loffler, I, Muller, CK, Leipner, C, Schultze-Mosgau, S, Stallmach, A, Kinne, RW, Wolf, G: TGF-beta and fibrosis in different organs - molecular pathway imprints. *Biochimica et biophysica acta,* 1792**:** 746-756, 2009.
30. Giannandrea, M, Parks, WC: Diverse functions of matrix metalloproteinases during fibrosis. *Disease models & mechanisms,* 7**:** 193-203, 2014.
31. Verbrugh, HA, Van Dijk, WC, Peters, R, Van Der Tol, ME, Verhoef, J: The role of Staphylococcus aureus cell-wall peptidoglycan, teichoic acid and protein A in the processes of complement activation and opsonization. *Immunology,* 37**:** 615-621, 1979.
32. Harboe, M, Garred, P, Lindstad, JK, Pharo, A, Muller, F, Stahl, GL, Lambris, JD, Mollnes, TE: The role of properdin in zymosan- and Escherichia coli-induced complement activation. *J Immunol,* 189**:** 2606-2613, 2012.
33. Lamouille, S, Xu, J, Derynck, R: Molecular mechanisms of epithelial-mesenchymal transition. *Nature reviews Molecular cell biology,* 15**:** 178-196, 2014.
34. Tang, S, Leung, JC, Chan, LY, Tsang, AW, Chen, CX, Zhou, W, Lai, KN, Sacks, SH: Regulation of complement C3 and C4 synthesis in human peritoneal mesothelial cells by peritoneal dialysis fluid. *Clinical and experimental immunology,* 136**:** 85-94, 2004.
35. Young, GA, Kendall, S, Brownjohn, AM: Complement activation during CAPD. *Nephrology, dialysis, transplantation : official publication of the European Dialysis and Transplant Association - European Renal Association,* 8**:** 1372-1375, 1993.
36. Reddingius, RE, Schroder, CH, Daha, MR, Willems, HL, Koster, AM, Monnens, LA: Complement in serum and dialysate in children on continuous ambulatory peritoneal dialysis. *Peritoneal dialysis international : journal of the International Society for Peritoneal Dialysis,* 15**:** 49-53, 1995.
37. Yewdall, VM, Boscoe, MJ, Bennett-Jones, DN, Cameron, JS: Clinical applications of crossed immunoelectrophoresis to the study of complement activation. *Journal of clinical & laboratory immunology,* 24**:** 51-56, 1987.

38. Kim, S, Kim, SY, Pribis, JP, Lotze, M, Mollen, KP, Shapiro, R, Loughran, P, Scott, MJ, Billiar, TR: Signaling of high mobility group box 1 (HMGB1) through toll-like receptor 4 in macrophages requires CD14. *Mol Med,* 19**:** 88-98, 2013.
39. Huebener, P, Schwabe, RF: Regulation of wound healing and organ fibrosis by toll-like receptors. *Biochimica et biophysica acta,* 1832**:** 1005-1017, 2013.
40. Cao, S, Li, S, Li, H, Xiong, L, Zhou, Y, Fan, J, Yu, X, Mao, H: The potential role of HMGB1 release in peritoneal dialysis-related peritonitis. *PloS one,* 8**:** e54647, 2013.
41. LeBouder, E, Rey-Nores, JE, Rushmere, NK, Grigorov, M, Lawn, SD, Affolter, M, Griffin, GE, Ferrara, P, Schiffrin, EJ, Morgan, BP, Labeta, MO: Soluble forms of Toll-like receptor (TLR)2 capable of modulating TLR2 signaling are present in human plasma and breast milk. *J Immunol,* 171**:** 6680-6689, 2003.
42. Raby, AC, Le Bouder, E, Colmont, C, Davies, J, Richards, P, Coles, B, George, CH, Jones, SA, Brennan, P, Topley, N, Labeta, MO: Soluble TLR2 reduces inflammation without compromising bacterial clearance by disrupting TLR2 triggering. *J Immunol,* 183**:** 506-517, 2009.
43. Catalan, MP, Esteban, J, Subira, D, Egido, J, Ortiz, A, Grupo de Estudios Peritoneales de Madrid, FI: Inhibition of caspases improves bacterial clearance in experimental peritonitis. *Peritoneal dialysis international : journal of the International Society for Peritoneal Dialysis,* 23**:** 123-126, 2003.
44. Hohlbaum, AM, Gregory, MS, Ju, ST, Marshak-Rothstein, A: Fas ligand engagement of resident peritoneal macrophages in vivo induces apoptosis and the production of neutrophil chemotactic factors. *J Immunol,* 167**:** 6217-6224, 2001.
45. Garosi, G, Di Paolo, N: Morphological aspects of peritoneal sclerosis. *Journal of nephrology,* 14 Suppl 4**:** S30-38, 2001.
46. Garosi, G, Di Paolo, N: Pathophysiology and morphological clinical correlation in experimental and peritoneal dialysis-induced peritoneal sclerosis. *Advances in peritoneal dialysis Conference on Peritoneal Dialysis,* 16**:** 204-207, 2000.
47. Schneble, F, Bonzel, KE, Waldherr, R, Bachmann, S, Roth, H, Scharer, K: Peritoneal morphology in children treated by continuous ambulatory peritoneal dialysis. *Pediatric nephrology,* 6**:** 542-546, 1992.
48. Tomino, Y: Mechanisms and interventions in peritoneal fibrosis. *Clinical and experimental nephrology,* 16**:** 109-114, 2012.
49. Lai, KN, Lai, KB, Lam, CW, Chan, TM, Li, FK, Leung, JC: Changes of cytokine profiles during peritonitis in patients on continuous ambulatory peritoneal dialysis. *American journal of kidney diseases : the official journal of the National Kidney Foundation,* 35**:** 644-652, 2000.
50. Yung, S, Chan, TM: Pathophysiological changes to the peritoneal membrane during PD-related peritonitis: the role of mesothelial cells. *Mediators of inflammation,* 2012**:** 484167, 2012.
51. Spiller, S, Elson, G, Ferstl, R, Dreher, S, Mueller, T, Freudenberg, M, Daubeuf, B, Wagner, H, Kirschning, CJ: TLR4-induced IFN-gamma production increases TLR2 sensitivity and drives Gram-negative sepsis in mice. *J Exp Med,* 205**:** 1747-1754, 2008.
52. Lima, CX, Souza, DG, Amaral, FA, Fagundes, CT, Rodrigues, IP, Alves-Filho, JC, Kosco-Vilbois, M, Ferlin, W, Shang, L, Elson, G, Teixeira, MM: Therapeutic Effects of Treatment with Anti-TLR2 and Anti-TLR4 Monoclonal Antibodies in Polymicrobial Sepsis. *PloS one,* 10**:** e0132336, 2015.
53. Fassett, RG, Driver, R, Healy, H, Coombes, JS: Cardiovascular disease in peritoneal dialysis patients. *Panminerva medica,* 51**:** 151-161, 2009.
54. Walsh, PS, Metzger, DA, Higushi, R: Chelex 100 as a medium for simple extraction of DNA for PCR-based typing from forensic material. BioTechniques 10(4): 506-13 (April 1991). *BioTechniques,* 54**:** 134-139, 2013.
55. Rey Nores, JE, Bensussan, A, Vita, N, Stelter, F, Arias, MA, Jones, M, Lefort, S, Borysiewicz, LK, Ferrara, P, Labeta, MO: Soluble CD14 acts as a negative regulator of human T cell activation and function. *Eur J Immunol,* 29**:** 265-276, 1999.
56. Hurst, SM, Wilkinson, TS, McLoughlin, RM, Jones, S, Horiuchi, S, Yamamoto, N, Rose-John, S, Fuller, GM, Topley, N, Jones, SA: Il-6 and its soluble receptor orchestrate a temporal switch in the pattern of leukocyte recruitment seen during acute inflammation. *Immunity,* 14**:** 705-714, 2001.

57. Durieux, JJ, Vita, N, Popescu, O, Guette, F, Calzada-Wack, J, Munker, R, Schmidt, RE, Lupker, J, Ferrara, P, Ziegler-Heitbrock, HW, et al.: The two soluble forms of the lipopolysaccharide receptor, CD14: characterization and release by normal human monocytes. *Eur J Immunol,* 24**:** 2006-2012, 1994.

Table 1. Effect of blocking TLR2 in uremic peritoneal leukocytes on *S. epidermidis*-induced fibrosis-related gene expression.*

		S. epidermidis		*S. epidermidis* + anti-TLR2		Anti- TLR2 modulatory effect (%)***
Gene symbol	**Description**	**Fold Change ****	***P*-value ****	**Fold Change****	***P*-value ****	
Ccl11	Chemokine (C-C motif) ligand 11	**0.5**	0.018	0.7	0.137	**-34.7**
Ccl2	Chemokine (C-C motif) ligand 2	**12.0**	0.001	14.5	0.001	22.5
Ccl3	Chemokine (C-C motif) ligand 3, MIP1a	**16.5**	0.001	3.2	0.065	**-86.0**
Ccr2	Chemokine (C-C motif) receptor 2	**0.3**	0.010	0.4	0.015	-11.2
Ctgf	Connective tissue growth factor	**0.4**	0.048	0.4	0.040	-
Edn1	Endothelin 1	**14.9**	0.001	11.0	0.006	**-28.2**
Grem1	Gremlin 1	**0.2**	0.001	0.4	0.001	-13.6
Ifng	Interferon gamma	**55.2**	0.001	63.5	0.001	15.4
Il10	Interleukin 10	**240.8**	0.001	188.9	0.001	**-21.7**
Il13	Interleukin 13	**10.1**	0.026	9.5	0.047	-5.6
Il1a	Interleukin 1, alpha	**19.7**	0.001	18.9	0.001	-4.0
Il1b	Interleukin 1, beta	**31.8**	0.011	30.1	0.004	-5.5
Itga1	Integrin, alpha 1	**9.5**	0.001	9.4	0.001	-1.9
ItgaV	Integrin, alpha V	**2.6**	0.004	3.3	0.002	40.7
Itgb3	Integrin, beta 3	**5.7**	0.001	6.6	0.002	17.6
Itgb5	Integrin, beta 5	**0.3**	0.001	0.3	0.004	-
Itgb8	Integrin, beta 8	**12.6**	0.004	13.7	0.011	9.4
Mmp1	Matrix metallopeptidase 1	**67.1**	0.001	61.1	0.001	-9.0
Mmp14	Matrix metallopeptidase 14	**3.6**	0.013	2.6	0.203	**-38.9**
Mmp3	Matrix metallopeptidase 3	**5.5**	0.001	3.6	0.001	**-41.7**
Mmp8	Matrix metallopeptidase 8	**3.5**	0.001	4.7	0.002	44.8
Plg	Plasminogen	**2.8**	0.031	1.0	0.903	**-100.0**
Serpina1	Serpin peptidase inhibitor, clade A	**9.7**	0.001	8.8	0.001	-10.3
Snai1	Snail homolog 1	**7.2**	0.049	5.3	0.063	**-31.2**
Stat1	Signal transducer and activator of transcription 1, 91kDa	**2.5**	0.010	2.6	0.012	10.9
Tgif1	TGFB-induced factor homeobox 1	**2.3**	0.032	2.3	0.041	-
Timp3	TIMP metallopeptidase inhibitor 3	**0.3**	0.001	0.3	0.001	-
Timp4	TIMP metallopeptidase inhibitor 4	**0.4**	0.021	0.4	0.022	-
Tnf	Tumor necrosis factor	**4.9**	0.002	4.7	0.001	-6.5
Vegfa	Vascular endothelial growth factor A	**6.8**	0.001	6.8	0.001	-

*****Only statistically significant (*P*<0.05) *S. epidermidis*-induced ≤ 0.5 (bold gold) or ≥ 2 (bold red) fold changes were considered.

******Compared to Control group.

*******Compared to the effect of *S. epidermidis* treatment. Genes affected ≥20% are shown in blue (inhibition) or green (upregulation).

Table 2. Effect of blocking TLR2 in uremic peritoneal leukocytes on non-infected PD effluent-induced fibrosis-related gene expression.*

		Non-infected PDE		Non-infected PDE + anti-TLR2		Anti- TLR2 modulatory effect (%)***
Gene symbol	**Description**	**Fold Change ****	***P*-value ****	**Fold Change****	***P*-value ****	
Ccl2	Chemokine (C-C motif) ligand 2	**2.2**	0.017	1.1	0.883	**-91.0**
Egf	Epidermal growth factor	**6.5**	0.001	1.1	0.835	**-98.9**
Il13	Interleukin 13	**3.5**	0.001	3.9	0.011	16.8
Il13ra2	Interleukin 13 receptor, alpha 2	**7.3**	0.002	6.7	0.004	-8.3
Il4	Interleukin 4	**4.2**	0.001	3.8	0.014	-11.2
Mmp13	Matrix metallopeptidase 13	**4.1**	0.001	1.1	0.835	**-98.0**
Smda3	SMAD family member 3	**0.4**	0.019	0.2	0.005	31.0

*****Only statistically significant (*P*<0.05) PDE#1-induced ≤ 0.5 (bold gold) or ≥ 2 (bold red) fold changes were considered.

******Compared to Control group.

*******Compared to the effect of *S. epidermidis* treatment. Genes affected ≥20% are shown in blue (inhibition) or green (upregulation).

Table 3. Changes in fibrosis-related peritoneal gene expression at day 28 in mice infected with *S. epidermidis* or *S. epidermidis* + sTLR2.*

		S. epidermidis		*S. epidermidis* + sTLR2		sTLR2 modulatory effect (%)***
Gene symbol	**Description**	**Fold Change ****	***P*-value ****	**Fold Change****	***P*-value ****	
Ccl12	Chemokine (C-C motif) ligand 12, MCP5	**12.4**	0.008	9.4	0.023	**-26.0**
Ccl3	Chemokine (C-C motif) ligand 3, MIP1a	**4.3**	0.033	5.2	0.005	25.8
Ccr2	Chemokine (C-C motif) receptor 2	**4.2**	0.043	2.5	0.082	**-53.7**
Cxcr4	Chemokine (C-X-C motif) receptor 4	**2.1**	0.036	1.7	0.113	**-31.4**
Fasl	Fas ligand (TNF superfamily, member 6)	**8.0**	0.048	3.2	0.209	**-68.1**
Hgf	Hepatocyte growth factor	**9.8**	0.048	3.7	0.050	**-69.6**
Ifng	Interferon gamma	**14.1**	0.018	15.2	0.004	8.4
Il10	Interleukin 10	**8.7**	0.010	2.5	0.001	**-80.2**
Il1b	Interleukin 1 beta	**7.8**	0.046	5.5	0.049	**-34.0**
Il6	Interleukin 6	**3.1**	0.001	1.4	0.218	**-79.3**
Itga2	Integrin alpha 2	**5.4**	0.019	3.6	0.076	**-41.9**
Itgb3	Integrin beta 3	**2.2**	0.001	1.6	0.001	**-47.9**
Mmp13	Matrix metallopeptidase 13	**4.4**	0.037	1.5	0.344	**-84.0**
Myc	Myelocytomatosis oncogene	**2.1**	0.005	1.7	0.078	**-41.7**
Serpine1	Serine (or cysteine) peptidase inhibitor, clade E, member 1	**3.5**	0.022	2.1	0.002	**-55.2**
Smad2	MAD homolog 2 (Drosophila)	**2.0**	0.018	1.4	0.037	**-58.8**
Sp1	Trans-acting transcription factor 1	**2.2**	0.002	1.5	0.046	**-58.8**
Stat1	Signal transducer and activator of transcription 1	**8.1**	0.046	6.4	0.041	**-24.0**
Tgfbr1	Transforming growth factor, beta receptor I	**2.3**	0.001	1.6	0.101	**-53.1**
Timp1	Tissue inhibitor of metalloproteinase 1	**3.2**	0.028	1.5	0.233	**-76.3**
Tnf	Tumor necrosis factor	**8.1**	0.042	14.3	0.043	88.5

*****Only statistically significant ($P<0.05$) *S. epidermidis*-induced ≤ 0.5 or ≥ 2 fold changes were considered.

******Compared to Control group.

*******Compared to the effect of *S. epidermidis* treatment. Genes affected ≥20% are shown in blue (inhibition) or green (upregulation).

Table 4. Changes in fibrosis-related peritoneal gene expression at day 49 in mice infected with *S. epidermidis* or *S. epidermidis* + sTLR2.

		S. epidermidis		*S. epidermidis* + sTLR2		sTLR2 modulatory effect (%)**
Gene symbol	**Description**	**Fold Change ***	***P*-value ***	**Fold Change***	***P*-value ***	
Fasl	Fas ligand (TNF superfamily, member 6)	**2.6**	0.236	0.9	0.907	-105.2
Mmp1a	Matrix metallopeptidase 1a (interstitial collagenase)	**0.5**	0.001	0.7	0.207	-48.1
Mmp3	Matrix metallopeptidase 3	**0.4**	0.011	0.9	0.506	-87.7
Mmp9	Matrix metallopeptidase 9	**0.4**	0.024	0.5	0.019	-16.6
Timp1	Tissue inhibitor of metalloproteinase 1	0.6	0.220	0.3	0.036	N/A

*****Compared to Control group.

******Compared to the effect of *S. epidermidis* treatment.

N/A, not applicable.

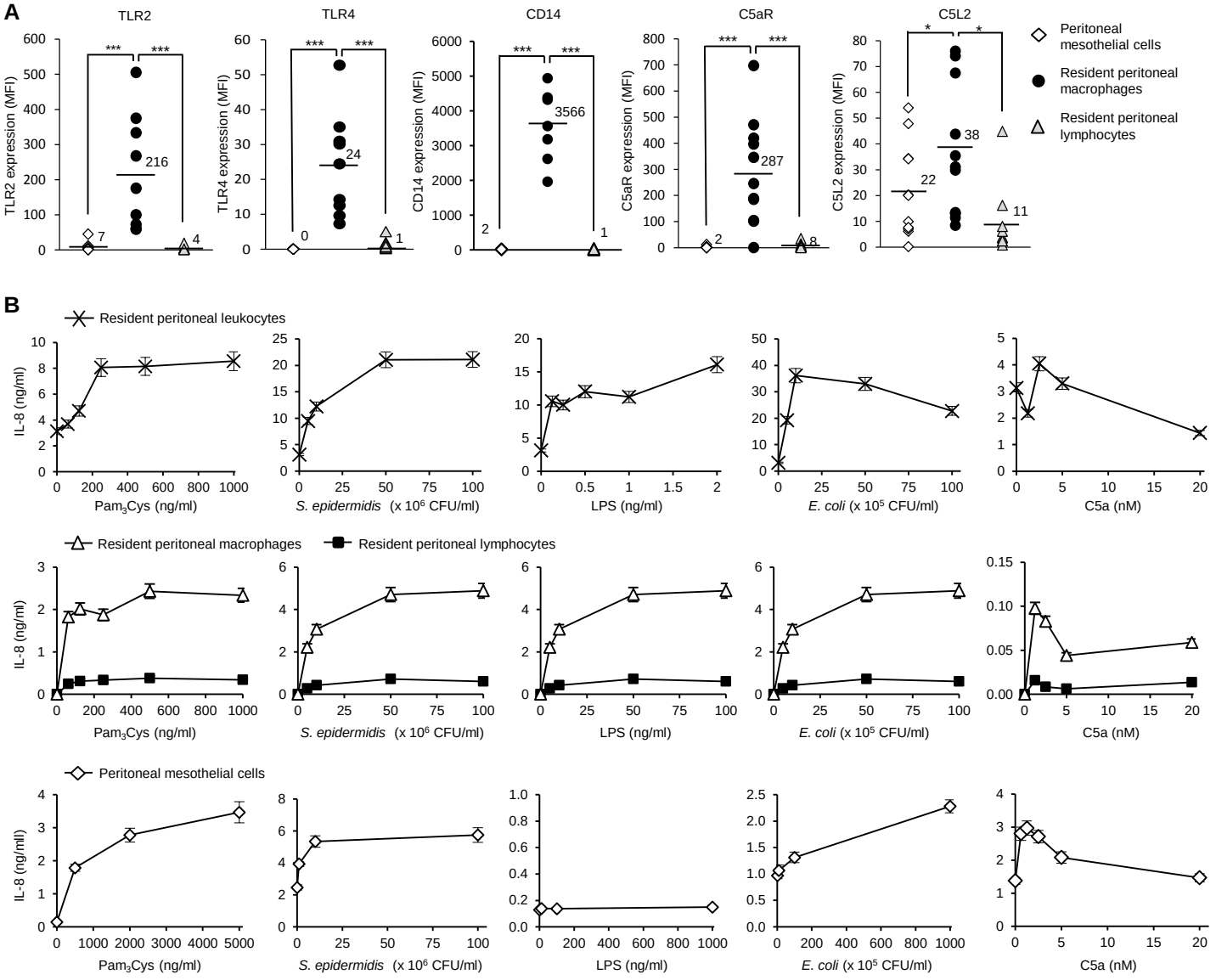

Figure 1. Peritoneal leukocytes and mesothelial cells differentially express TLR2, TLR4 and C5aR and respond to TLR agonists or C5a. (A) Expression levels of TLR2, TLR4, C5aR, the TLR co-receptor CD14 and the C5aR negative regulator C5L2 in PDE-isolated resident peritoneal macrophages, lymphocytes and peritoneal mesothelial cells (from omentum), as determined by flow cytometry. Results are from the analysis of cells isolated from PDE or omentum of 7 to 10 different donors. *, $P<0.05$; ***, $P<0.005$. (B) IL-8 levels in culture supernatants of resident peritoneal leukocytes, macrophages, lymphocytes and peritoneal mesothelial cells stimulated overnight with the indicated concentrations of various TLR agonists or C5a. Leukocytes, macrophages and lymphocytes were from the same patient sample. Results shown are the mean (± SD) from one experiment representative of three performed with cells from different donors.

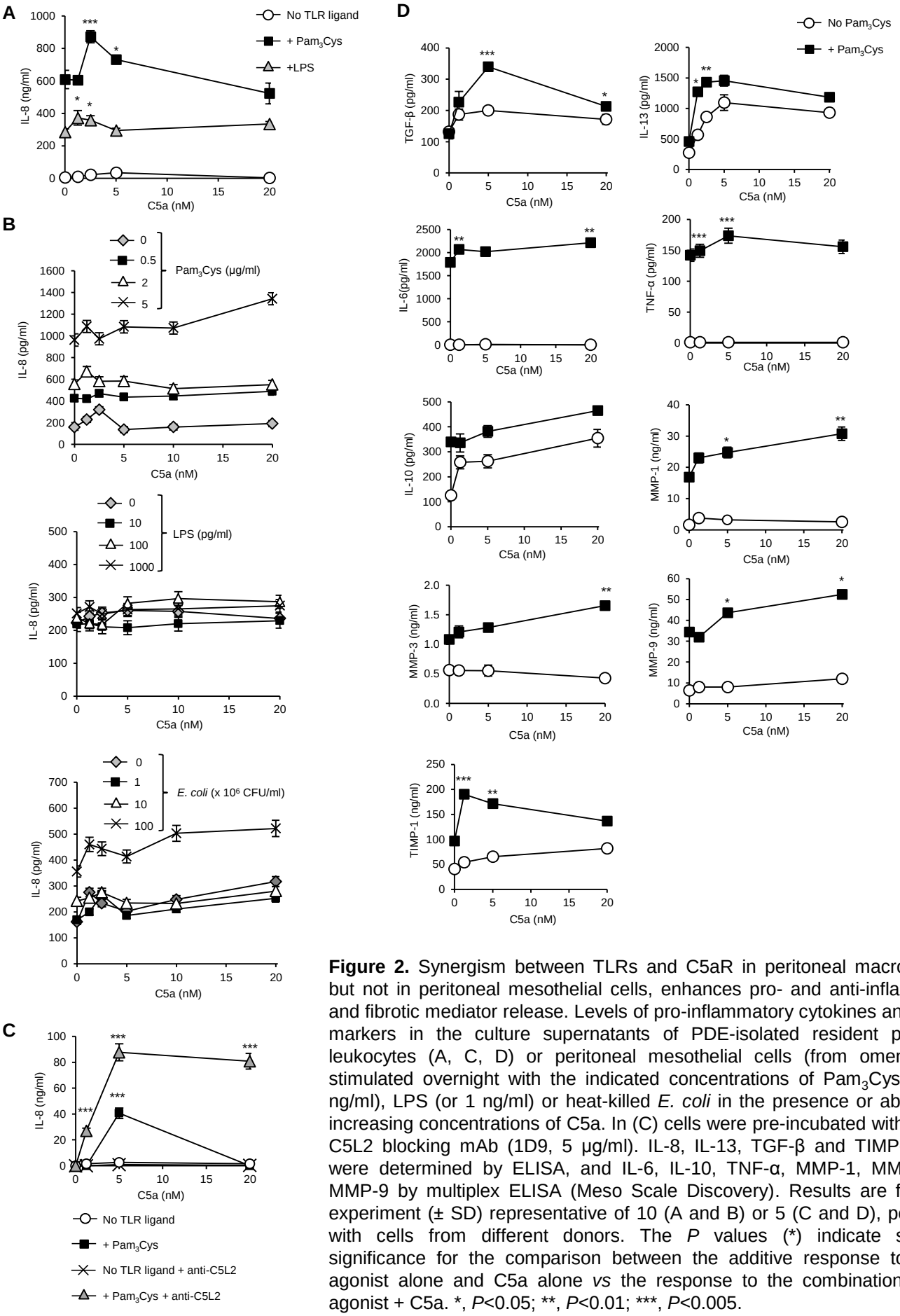

Figure 2. Synergism between TLRs and C5aR in peritoneal macrophages, but not in peritoneal mesothelial cells, enhances pro- and anti-inflammatory and fibrotic mediator release. Levels of pro-inflammatory cytokines and fibrotic markers in the culture supernatants of PDE-isolated resident peritoneal leukocytes (A, C, D) or peritoneal mesothelial cells (from omentum, B) stimulated overnight with the indicated concentrations of Pam_3Cys (or 250 ng/ml), LPS (or 1 ng/ml) or heat-killed *E. coli* in the presence or absence of increasing concentrations of C5a. In (C) cells were pre-incubated with an anti-C5L2 blocking mAb (1D9, 5 µg/ml). IL-8, IL-13, TGF-β and TIMP-1 levels were determined by ELISA, and IL-6, IL-10, TNF-α, MMP-1, MMP-3 and MMP-9 by multiplex ELISA (Meso Scale Discovery). Results are from one experiment (± SD) representative of 10 (A and B) or 5 (C and D), performed with cells from different donors. The *P* values (*) indicate statistical significance for the comparison between the additive response to a TLR agonist alone and C5a alone *vs* the response to the combination of TLR agonist + C5a. *, $P<0.05$; **, $P<0.01$; ***, $P<0.005$.

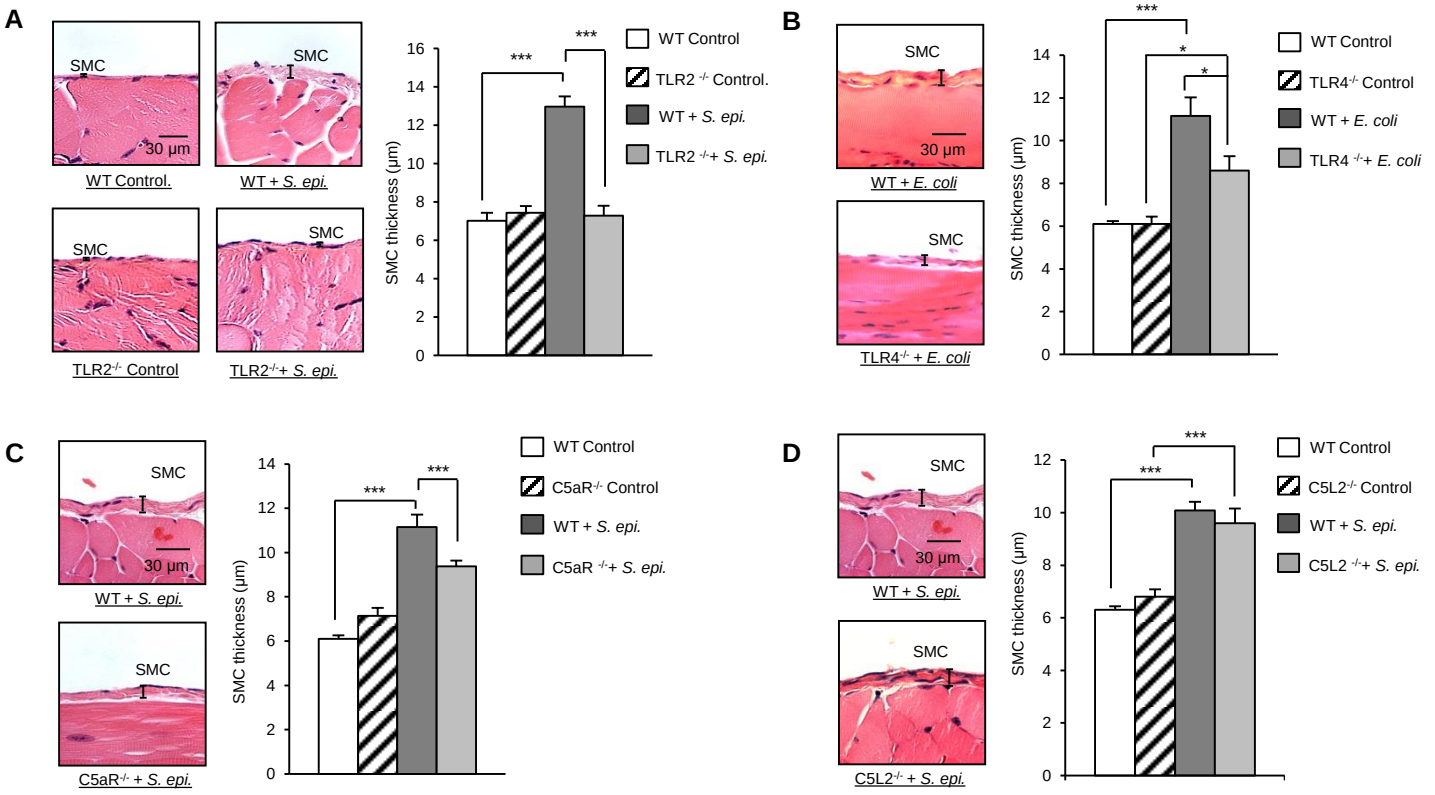

Figure 3. TLR2, TLR4, C5aR and C5L2 differentially contribute to bacteria-induced peritoneal fibrosis development in mouse peritonitis models. (A-D) Wild-type (WT), TLR2 deficient (TLR2$^{-/-}$), TLR4$^{-/-}$, C5aR$^{-/-}$ or C5L2$^{-/-}$ mice (n=5 per group) were inoculated intraperitoneally 4 times at weekly intervals with heat-killed *S. epidermidis* (*S. epi*., 5 x 10^8 CFU/mouse) or *Escherichia coli* (*E. coli*, *2* x 10^7 CFU/mouse), or left untreated (control). Four weeks after the last injection, histological analysis of the peritoneal membrane was conducted. Sections of peritoneal membrane (5 µm) were stained with haematoxylin/eosin and the thickness of the sub-mesothelial compact zone (SMC, layer between the muscle and membrane surface) was determined using the Leica Qwin imaging software. Representative fields (x40 magnification) are shown. Bar plots show the mean (± SEM) of SMC thickness in each experimental group. The mean of SMC was determined as described in Concise Methods. *, *P*<0.05; ***, *P*<0.005.

	Patient:	A	B	C
Urea (mM)	Blood	17.5	15.8	16.0
	PDE	15.9	14.2	15.4
Creatinine (µM)	Blood	418.0	547.3	618.0
	PDE	353.2	428.5	537.5

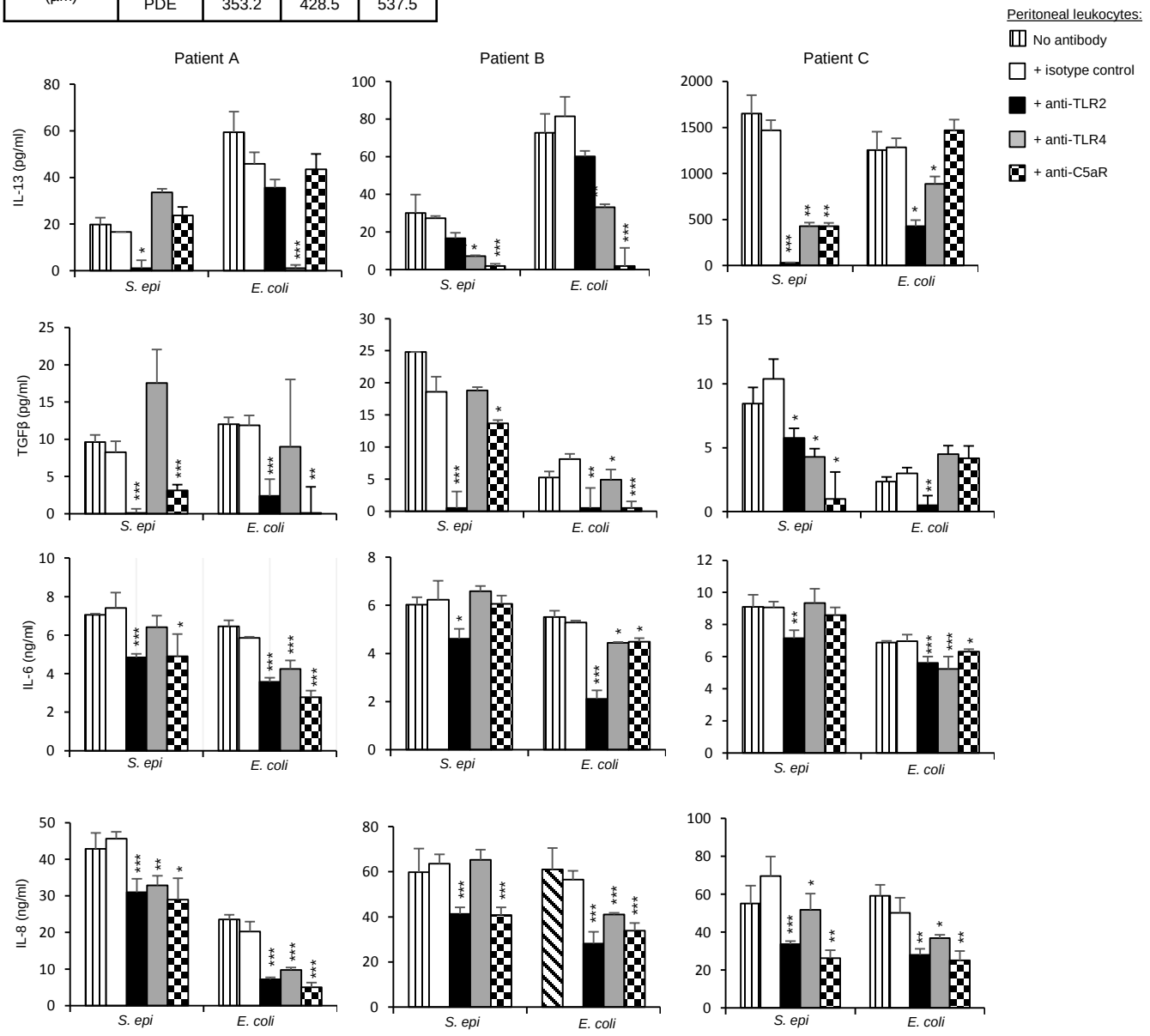

Figure 4. TLR2, TLR4 and C5aR are involved in bacteria-induced pro-fibrotic and inflammatory responses of peritoneal leukocytes from uremic PD patients. Levels of pro-fibrotic and inflammatory cytokines released by PDE-isolated uremic leukocytes cultured overnight with or without heat-killed *S. epidermidis* (10^7 cfu/ml) or *E. coli*. (10^6 cfu/ml) in the presence of the indicated blocking mAbs or isotype-matched control (5 µg/ml). To maintain the uremic milieu throughout the experiments, the culture medium was supplemented with the patients' own PDE (1/2 dilution). The uremic status of the patients was confirmed by urea and creatinine measurements in the blood and PDE (inset table). Results are the mean (± SD) of triplicates after background subtraction (cells cultured in the absence of bacteria, but presence of the blocking mAbs or isotype control, typically IL-8 < 1ng/ml, IL-6 < 100 pg/ml, IL-13 < 25 pg/ml, TGFβ < 10 pg/ml). *, *P*<0.05; **, *P* <0.01; ***, *P* <0.005 (specific mAb *vs* isotype control, Student's *t* test).

A

	Patient:	D	E	F
Urea (mM)	Blood	16.7	24.7	17.9
	PDE	19.4	22.0	12.7
Creatinine (µM)	Blood	437.0	498.0	491.0
	PDE	484.2	406.8	361.1

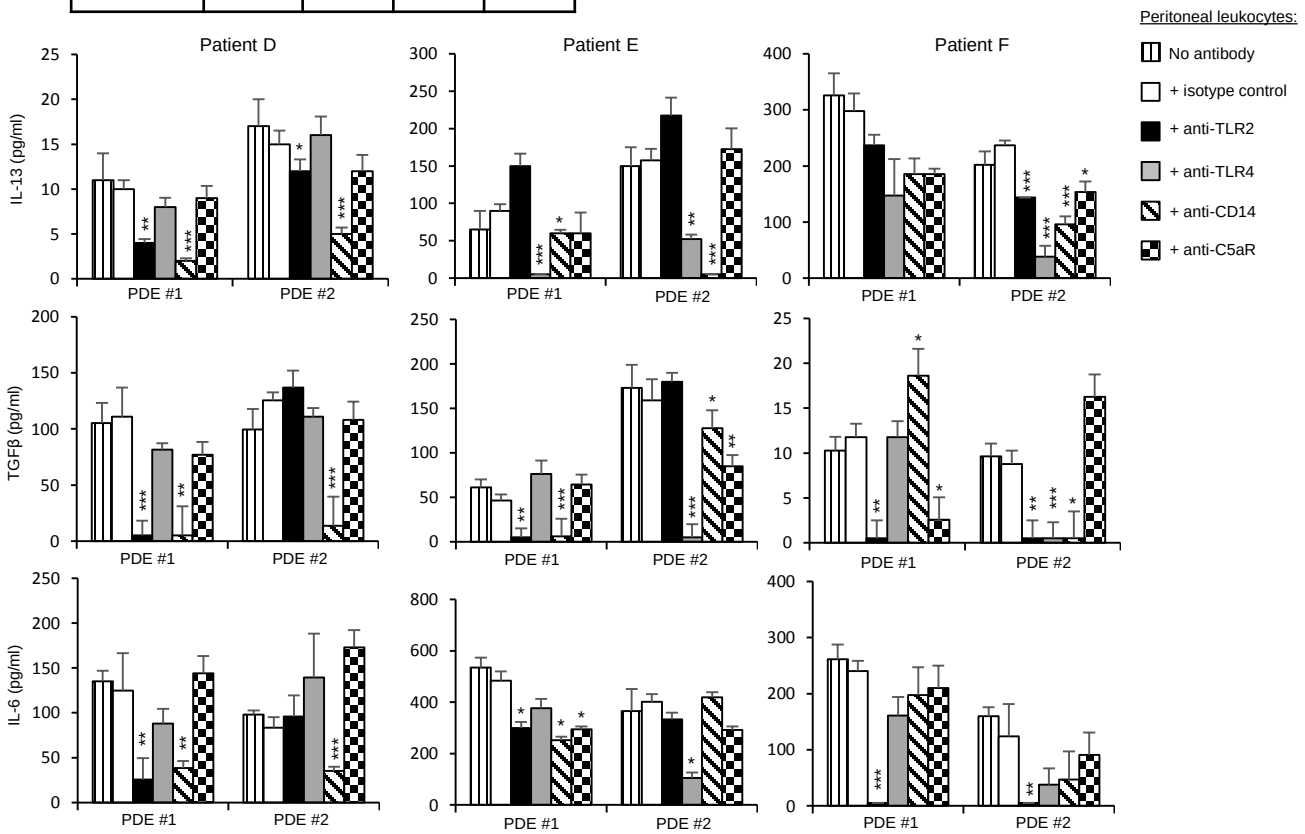

B

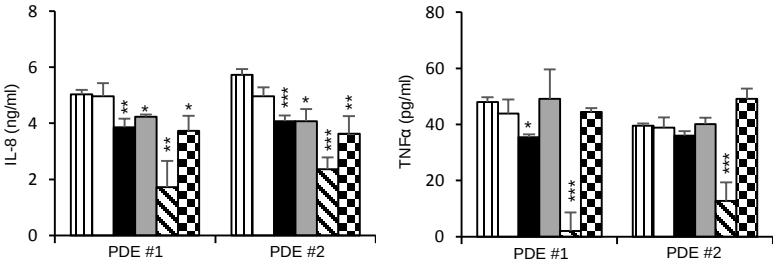

C

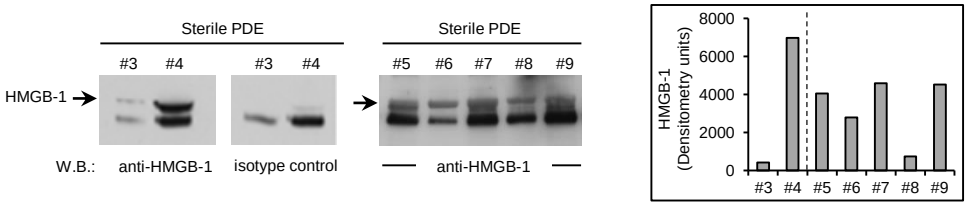

Figure 5. Differential involvement of TLR2, TLR4, CD14 and C5aR in PD-induced sterile peritoneal inflammation. (A) Levels of pro-fibrotic (A) and inflammatory (B) cytokines released by PDE-isolated uremic leukocytes stimulated (17h) with non-infected PDE (PDE #1: urea:16.6 mM, creatinine: 286.4 µM; PDE #2: urea: 15.8 mM, creatinine: 415.5 µM) in the presence of the indicated blocking mAbs or isotype-matched control (5 µg/ml). The non-infected PDEs used for stimulation also served to maintain uremic conditions throughout the experiment. The uremic status of the patients was confirmed by urea and creatinine measurements in the blood and PDE (A, inset table). Results are the mean (± SD) of triplicates after background subtraction (cells cultured in the absence of PDE, but presence of the mAbs, typically IL-8 < 1ng/ml, IL-6 < 100 pg/ml, IL-13 < 25 pg/ml, TGFβ < 10 pg/ml). *, P<0.05; **, P <0.01; ***, P <0.005 (specific mAb *vs* isotype control, Student's *t* test). Results in B are from patient D. (C) Western blot analysis and densitometric scanning of HMGB-1 detected in sterile PDE samples (diluted 20 times) from seven donors. Arrows point at the HMGB-1 protein specifically detected. The dashed line in the inset indicates separate gels.

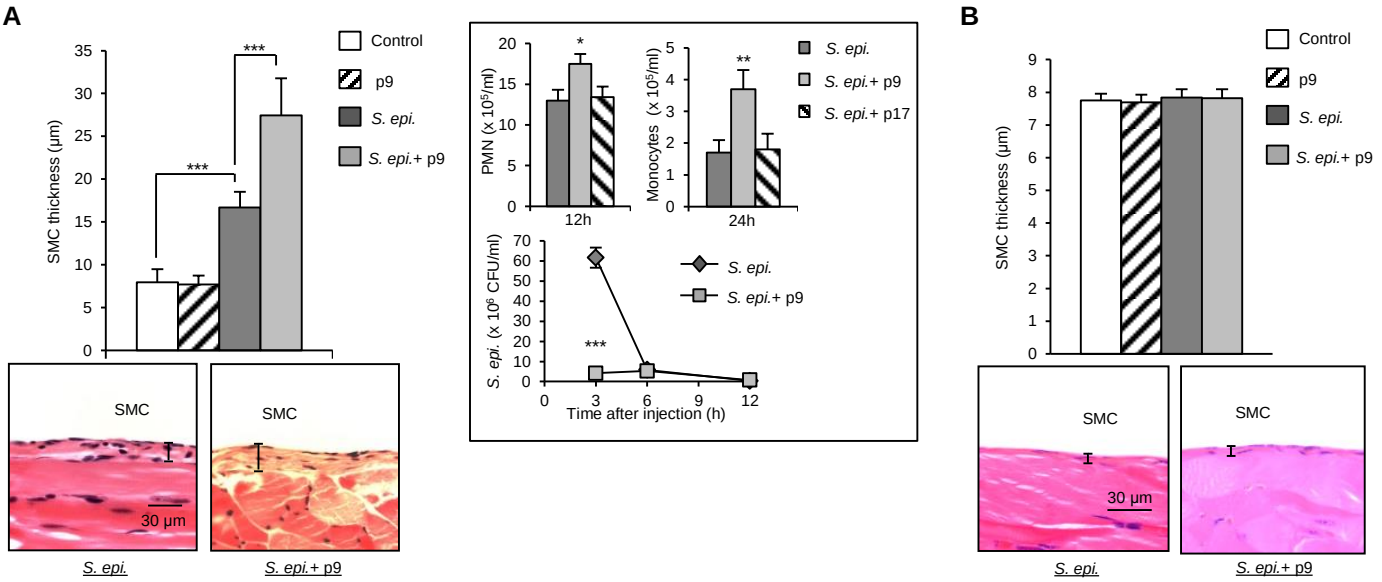

Figure 6. The intensity of the TLR-mediated inflammatory episodes, in addition to their number, impacts on peritoneal fibrosis development. C57BL/6J mice (n=5 per group) were inoculated intraperitoneally 4 times (A) or 2 times (B) at weekly intervals with live (A) or heat-killed (B) *S. epidermidis* (5 x 10^8 CFU/mouse) or PBS (control), in the presence or absence of a TLR2-derived peptide (p9 or control p17; 20 µg/mouse). Four weeks after the last injection, histological analysis of the peritoneal membrane was conducted as described for Figure 3. Representative fields (x40 magnification) are shown, and bar plots show the mean (± SEM) of the sub-mesothelial compact zone (SMC) thickness for each group. ***, *P*<0.005. (A, inset) At the indicated time points following the first injection, peritoneal lavages were obtained. PMN and monocyte numbers were determined by flow cytometry using anti-Ly6G and anti-7/4 specific monoclonal antibodies, and bacterial titers by overnight culture on microbiological agar plates.*, *P*<0.05; **, *P*<0.01; ***, *P*<0.005 (*S. epi.* + p9 *vs S. epi.* alone).

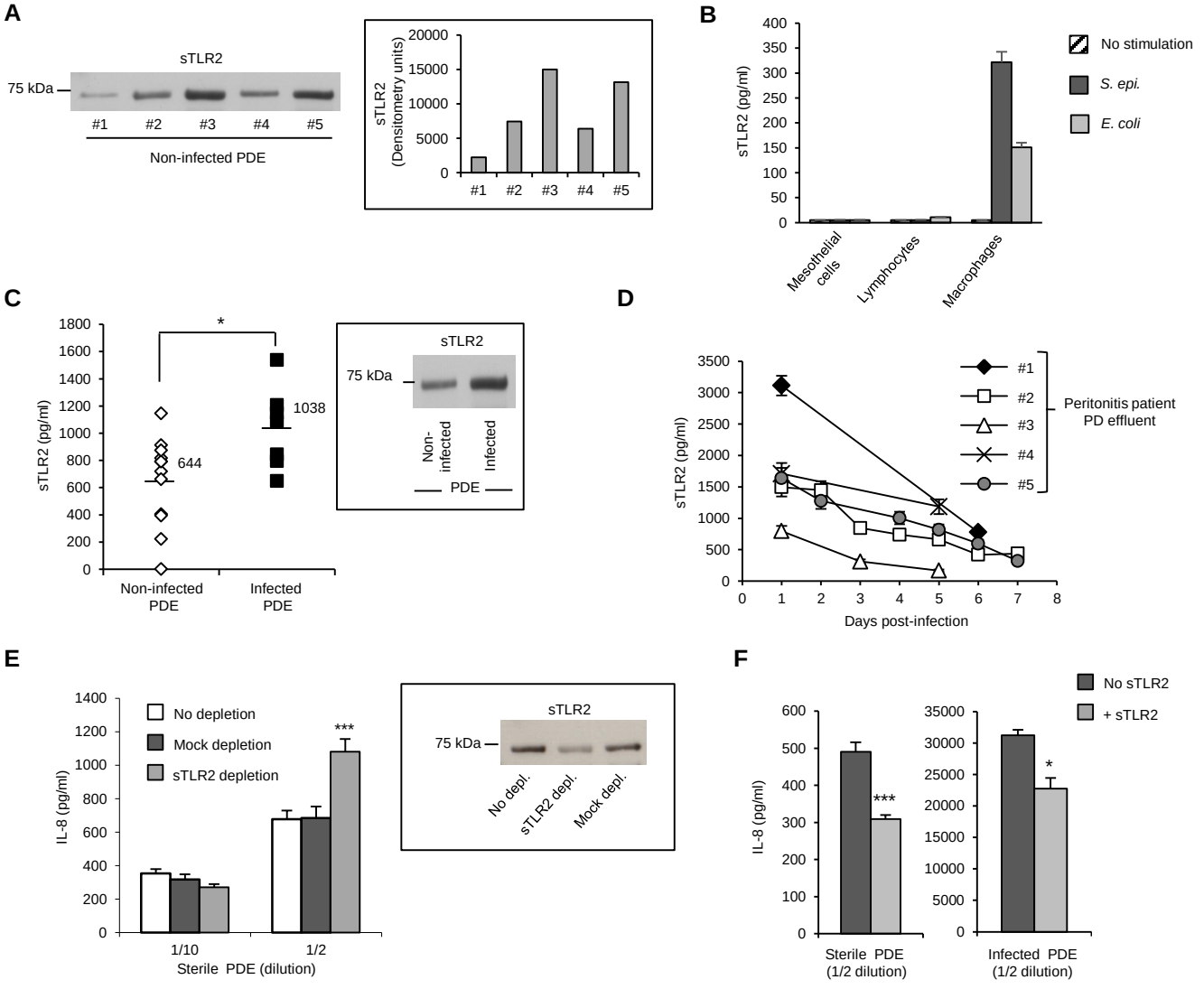

Figure 7. sTLR2 is present in PD effluent from non-infected patients and can reduce PD-induced pro-inflammatory responses *ex vivo*. (A) Western blot analysis and densitometric scanning of sTLR2 detected in sterile PDE from different donors. (B) Levels of sTLR2 in the culture supernatants of peritoneal mesothelial cells, sterile PDE-isolated lymphocytes and macrophages stimulated (16h) or not with heat-killed *S. epidermidis* (5 x 10^8 CFU/ml) or *E. coli* (5 x 10^7 CFU/ml). Results are from one experiment representative of three, performed with cells from different donors. (C and D) Levels of sTLR2 in PDE from patients without or with ongoing peritoneal infection tested at day 1 (C) or at the indicated times post-infection (D). Inset in (C) shows a representative sTLR2 Western blot profile in the PDE of one patient before and on day 1 of infection. In (D), results are expressed as means (± SD) for each time point. *, P <0.05. (E and F) Levels of IL-8 in the culture supernatant of PBMC (E) or PDE leukocytes (F) cultured overnight with the indicated dilutions of sterile or infected cell-free PDE depleted of sTLR2, mock-depleted or not depleted (E), or supplemented with 500 ng/ml of human recombinant sTLR2 (F). Depletion in (E) was ~80%, as estimated by Western Blot. Results are from one experiment (± SD) representative of three performed with cell-free PDE from different donors. *, P<0.05; ***, P<0.005 (sTLR2 depleted *vs* mock depleted or + sTLR2 *vs* no sTLR2).

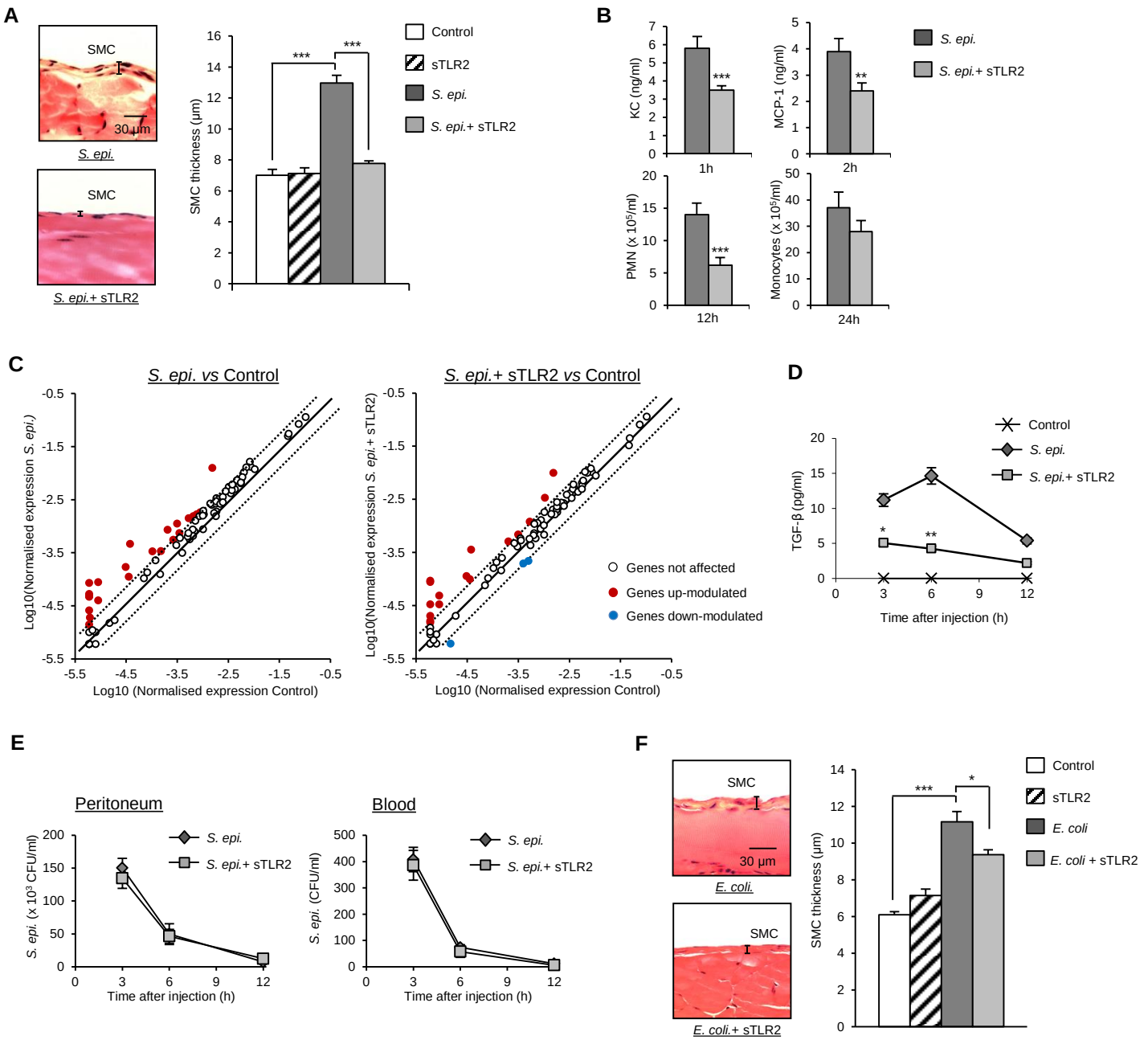

Figure 8. sTLR2 inhibits infection-induced peritoneal fibrosis development *in vivo*. (A-F) C57BL/6J mice (n=5 per group) were inoculated intraperitoneally 4 times at weekly intervals (A, C, F) or once (B, D, E) with live *S. epidermidis* (5 x 10^8 CFU/mouse, A-E) or heat-killed *Escherichia coli* (5 x 10^7 CFU/mouse, F) in the presence or absence of sTLR2 (250 ng/mouse). In (A and F), four weeks after the last injection (day 49), histological analysis of the peritoneal membrane was conducted as described for Figure 3. Representative fields (x40 magnification) are shown; bar plots show the mean (± SEM) of the sub-mesothelial compact zone (SMC) thickness for each group. In (B, D and E), the animals were sacrificed at the indicated time points after the injection and peritoneal lavages and blood were obtained. Cytokine levels were determined by ELISA, PMN and monocyte numbers by flow cytometry using anti-Ly6G and anti-7/4 specific monoclonal antibodies, and bacterial titers by overnight culture on microbiological agar plate. *, $P<0.05$; **, $P<0.01$; ***, $p<0.005$ (*S. epi* + sTLR2 *vs S. epi.* alone). In (C), scatter plots show the effect of sTLR2 on the *S. epidermidis*-induced modulation of fibrosis-related genes, as assessed by RT-qPCR on RNA extracted from peritoneal membranes one week after the fourth injection (day 28).

SUPPLEMENTAL MATERIAL

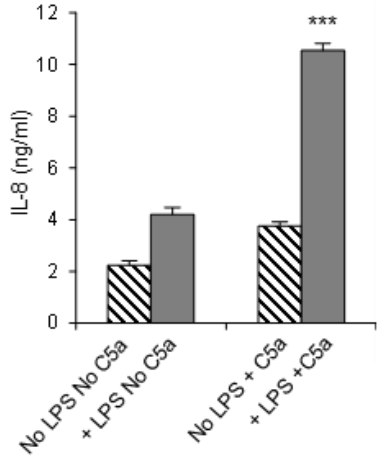

Figure 1. Co-stimulation via TLR4 and C5aR in peripheral blood mononuclear cells results in a synergistically enhanced pro-inflammatory response. Levels of IL-8 (ELISA) in the culture supernatant of PBMC (1.5 x 10^5 cells/ well in triplicates) cultured (14h) in the presence or absence of LPS (10 ng/ml) and C5a (2.5 nM). Synergism was assessed by comparing the additive response to each individual ligand (No LPS + C5a or + LPS No C5a) with that of the combination of ligands (+ LPS + C5a). Results are from one experiment (±SD) representative of three. ***, *P*< 0.005, C5a treatment + LPS treatment *vs* C5a + LPS treatment.

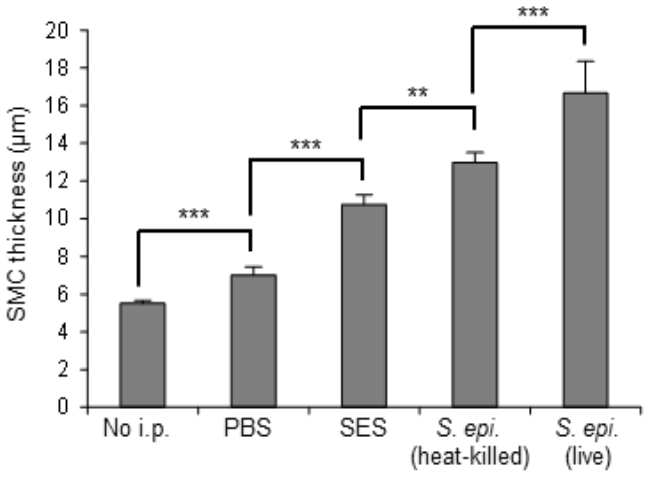

Figure 2. Repeated peritoneal inoculation of Gram-positive bacteria and bacterial components induces peritoneal fibrosis development in mice. Mice (n=5 per group) were intraperitoneally inoculated 4 times at weekly intervals with live or heat-killed *S. epidermidis* (5 x 10^8 CFU/mouse), a cell-free supernatant from *S. epidermidis* cultures (SES), PBS or left untreated (No i.p.). Four weeks after the last injection, histological analysis of the peritoneal membrane was conducted. Sections of peritoneal membrane (5 µm) were stained with haematoxylin/eosin and the thickness of the sub-mesothelial compact zone (SMC, layer between the muscle and membrane surface) was determined using the Leica Qwin imaging software. The mean of SMC was determined as described in Concise Methods. Three different fields of view were examined for each animal, 6 measurements were made per field and the average of the 10 highest measurements was taken as mean of SMC thickness. **, *P*<0.01; ***, *P*<0.005.

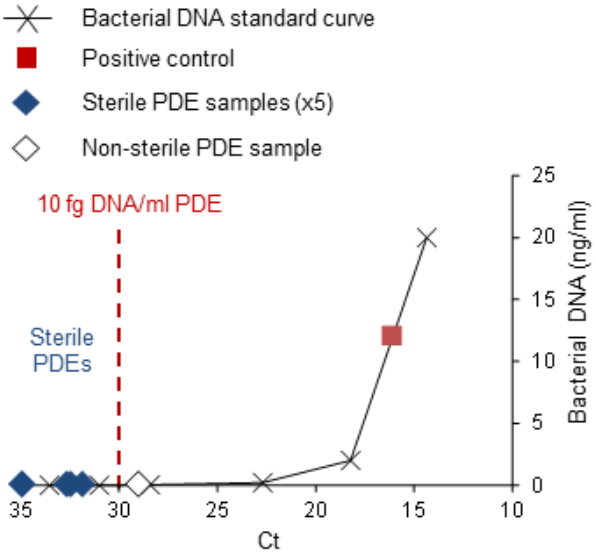

Figure 3. Testing for bacterial DNA in non-infected PD effluents. Total DNA was extracted from non-infected cell-free PDE by a chelex-based method as previously described[54]. One PDE sample was spiked with heat-killed *S. epidermidis* prior to extraction to serve as a positive control. Pan-bacterial DNA was then amplified by qPCR using the Femto™ Bacterial DNA Quantification kit (Zymo research), and the amount of DNA in PDE was determined using the kit's internal standard curve as a reference. A Ct of 30 cycles, corresponding to 10 fg of bacterial DNA per 1ml of PDE, was set as PDE sterility cut off. Representative examples of the Ct values obtained for non-infected PDE (blue diamonds) and positive controls (red square) are shown together with a typical standard curve.

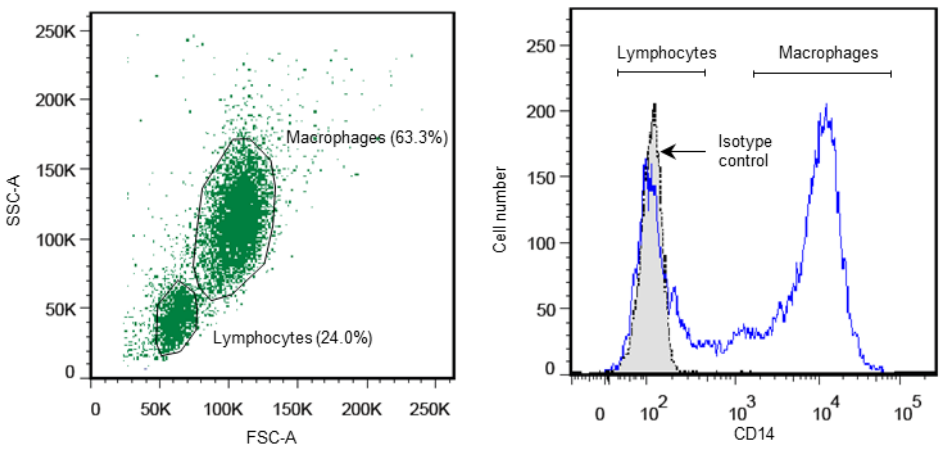

Figure 4. Flow cytometric analysis of leukocytes in non-infected PD effluents. Peritoneal leukocytes were prepared from non-infected PDE and analysed by flow cytometry as described in Concise Methods. The dot plot and fluorescence histogram show a representative forward and side scatter and the typical CD14 expression profile, respectively, of the total live peritoneal leukocyte population following dead cells exclusion (eFluor viability dye, <15%). Lymphocytes and macrophages (representative percentages shown) were identified based on their forward and side scatter profiles and CD14 expression levels.

Table 1. Effect of blocking TLR2 in uremic peritoneal leukocytes on *S. epidermidis*-induced fibrosis-related gene expression (complete array).*

		S. epidermidis		***S. epidermidis* + anti-TLR2**	
Gene symbol	**Description**	**Fold Change****	***P*-value****	**Fold Change****	***P*-value****
Acta2	Actin, alpha 2, smooth muscle, aorta	1.0	0.789	1.0	0.946
Agt	Angiotensinogen (serpin peptidase inhibitor, clade A, member 8)	1.0	0.757	1.0	0.903
Akt1	V-akt murine thymoma viral oncogene homolog 1	1.1	0.691	0.9	0.796
Bcl2	B-cell CLL/lymphoma 2	0.8	0.232	0.8	0.383
Bmp7	Bone morphogenetic protein 7	1.6	0.291	0.6	0.199
Cav1	Caveolin 1, caveolae protein, 22kDa	0.5	0.034	0.5	0.039
Ccl11	Chemokine (C-C motif) ligand 11	**0.5**	0.018	0.7	0.137
Ccl2	Chemokine (C-C motif) ligand 2	**12.0**	0.001	14.5	0.001
Ccl3	Chemokine (C-C motif) ligand 3	**16.5**	0.001	3.2	0.065
Ccr2	Chemokine (C-C motif) receptor 2	**0.3**	0.010	0.4	0.015
Cebpb	CCAAT/enhancer binding protein (C/EBP), beta	1.6	0.215	1.5	0.351
Col1a2	Collagen, type I, alpha 2	0.7	0.101	0.7	0.063
Col3a1	Collagen, type III, alpha 1	0.7	0.021	0.7	0.015
Ctgf	Connective tissue growth factor	**0.4**	0.048	0.4	0.040
Cxcr4	Chemokine (C-X-C motif) receptor 4	1.8	0.102	1.8	0.056
Dcn	Decorin	1.1	0.402	1.0	0.928
Edn1	Endothelin 1	**14.9**	0.001	11.0	0.006
Egf	Epidermal growth factor	1.0	0.757	1.0	0.903
Eng	Endoglin	0.5	0.011	0.5	0.016
Faslg	Fas ligand (TNF superfamily, member 6)	1.6	0.001	1.9	0.001
Grem1	Gremlin 1	**0.2**	0.001	0.4	0.001
Hgf	Hepatocyte growth factor (hepapoietin A; scatter factor)	0.6	0.026	0.5	0.020
Ifng	Interferon, gamma	**55.2**	0.001	63.5	0.001
Il10	Interleukin 10	**240.8**	0.001	188.9	0.001
Il13	Interleukin 13	**10.1**	0.026	9.5	0.047
Il13ra2	Interleukin 13 receptor, alpha 2	1.9	0.002	1.7	0.002
Il1a	Interleukin 1, alpha	**19.7**	0.001	18.9	0.001
Il1b	Interleukin 1, beta	**31.8**	0.011	30.1	0.004
Il4	Interleukin 4	1.0	0.757	1.0	0.903
Il5	Interleukin 5	1.3	0.221	0.4	0.035
Ilk	Integrin-linked kinase	1.5	0.049	1.3	0.199
Inhbe	inhibin, beta E	1.0	0.757	1.0	0.903
Itga1	Integrin, alpha 1	**9.5**	0.001	9.4	0.001
Itga2	Integrin, alpha 2	1.4	0.118	1.2	0.362
Itga3	Integrin, alpha 3	0.7	0.066	0.6	0.076
Itgav	Integrin, alpha V	**2.6**	0.004	3.3	0.002
Itgb1	Integrin, beta 1	1.3	0.266	1.4	0.180
Itgb3	Integrin, beta 3 (platelet glycoprotein IIIa, antigen CD61)	**5.7**	0.001	6.6	0.002
Itgb5	Integrin, beta 5	**0.3**	0.001	0.3	0.004
Itgb6	Integrin, beta 6	1.9	0.013	1.2	0.339
Itgb8	Integrin, beta 8	**12.6**	0.004	13.7	0.011
Jun	Jun proto-oncogene	0.9	0.628	0.9	0.930
Lox	Lysyl oxidase	1.0	0.841	0.9	0.478
Ltbp1	Latent transforming growth factor beta binding protein 1	0.6	0.134	0.6	0.209
Mmp1	Matrix metallopeptidase 1 (interstitial collagenase)	**67.1**	0.001	61.1	0.001
Mmp13	Matrix metallopeptidase 13 (collagenase 3)	1.0	0.757	1.0	0.903
Mmp14	Matrix metallopeptidase 14 (membrane-inserted)	**3.6**	0.013	2.6	0.203
Mmp2	Matrix metallopeptidase 2 (gelatinase A)	2.0	0.008	1.7	0.022
Mmp3	Matrix metallopeptidase 3 (stromelysin 1, progelatinase)	**5.5**	0.001	3.6	0.001
Mmp8	Matrix metallopeptidase 8 (neutrophil collagenase)	**3.5**	0.001	4.7	0.002
Mmp9	Matrix metallopeptidase 9 (gelatinase B)	0.7	0.035	0.8	0.260
Myc	V-myc myelocytomatosis viral oncogene homolog (avian)	0.9	0.728	0.8	0.012
Nfkb1	Nuclear factor of kappa light polypeptide gene enhancer in B-cells 1	1.5	0.228	1.7	0.140
Pdgfa	Platelet-derived growth factor alpha polypeptide	1.8	0.013	2.2	0.009
Pdgfb	Platelet-derived growth factor beta polypeptide	0.9	0.674	1.2	0.599
Plat	Plasminogen activator, tissue	**0.2**	0.092	0.2	0.086
Plau	Plasminogen activator, urokinase	1.1	0.828	1.1	0.712
Plg	Plasminogen	**2.8**	0.031	1.0	0.903
Serpina1	Serpin peptidase inhibitor, clade A, member 1	**9.7**	0.001	8.8	0.001

Serpine1	Serpin peptidase inhibitor, clade E, member 1	1.7	0.035	1.5	0.095
Serpinh1	Serpin peptidase inhibitor, clade H (heat shock protein 47), member 1	1.2	0.002	1.2	0.094
Smad2	SMAD family member 2	1.3	0.099	1.3	0.111
Smad3	SMAD family member 3	0.6	0.281	0.5	0.193
Smad4	SMAD family member 4	1.4	0.320	1.4	0.304
Smad6	SMAD family member 6	0.6	0.007	0.3	0.001
Smad7	SMAD family member 7	1.0	0.979	1.0	0.961
Snai1	Snail homolog 1 (Drosophila)	**7.2**	0.049	5.3	0.063
Sp1	Sp1 transcription factor	1.0	0.894	1.4	0.135
Stat1	Signal transducer and activator of transcription 1, 91kDa	**2.5**	0.010	2.6	0.012
Stat6	Signal transducer and activator of transcription 6, interleukin-4 induced	1.0	0.915	1.1	0.619
Tgfb1	Transforming growth factor, beta 1	0.7	0.032	0.6	0.052
Tgfb2	Transforming growth factor, beta 2	1.4	0.077	1.4	0.066
Tgfb3	Transforming growth factor, beta 3	2.0	0.015	2.1	0.060
Tgfbr1	Transforming growth factor, beta receptor 1	0.9	0.589	0.8	0.515
Tgfbr2	Transforming growth factor, beta receptor II (70/80kDa)	**0.4**	0.064	0.4	0.066
Tgif1	TGFB-induced factor homeobox 1	**2.3**	0.032	2.3	0.041
Thbs1	Thrombospondin 1	0.7	0.126	0.5	0.035
Thbs2	Thrombospondin 2	0.8	0.143	0.5	0.018
Timp1	TIMP metallopeptidase inhibitor 1	1.9	0.093	1.6	0.193
Timp2	TIMP metallopeptidase inhibitor 2	0.6	0.093	0.6	0.118
Timp3	TIMP metallopeptidase inhibitor 3	**0.3**	0.001	0.3	0.001
Timp4	TIMP metallopeptidase inhibitor 4	**0.4**	0.021	0.4	0.022
Tnf	Tumor necrosis factor	**4.9**	0.002	4.7	0.001
Vegfa	Vascular endothelial growth factor A	**6.8**	0.001	6.8	0.000

*****Statistically significant (P<0.05) and biologically relevant (≤ 0.5, bold gold or ≥ 2, bold red) *S. epidermidis*-induced fold changes are analysed in Results, Table 1

******Compared to Control group.

Table 2. Effect of blocking TLR2 in uremic peritoneal leukocytes on non-infected PDE-induced fibrosis-related gene expression (complete array).*

		Non-infected PDE		Non-infected PDE + anti-TLR2	
Gene symbol	**Description**	**Fold Change****	***P*-value****	**Fold Change****	***P*-value****
Acta2	Actin, alpha 2, smooth muscle, aorta	1.0	0.886	1.0	0.836
Agt	Angiotensinogen (serpin peptidase inhibitor, clade A, member 8)	0.8	0.291	1.1	0.835
Akt1	V-akt murine thymoma viral oncogene homolog 1	0.7	0.007	0.7	0.025
Bcl2	B-cell CLL/lymphoma 2	0.7	0.001	0.5	0.001
Bmp7	Bone morphogenetic protein 7	1.8	0.175	1.2	0.844
Cav1	Caveolin 1, caveolae protein, 22kDa	1.0	0.843	1.5	0.011
Ccl11	Chemokine (C-C motif) ligand 11	1.3	0.490	1.1	0.835
Ccl2	Chemokine (C-C motif) ligand 2	**2.2**	0.017	1.1	0.883
Ccl3	Chemokine (C-C motif) ligand 3	0.6	0.001	0.3	0.001
Ccr2	Chemokine (C-C motif) receptor 2	1.3	0.014	0.9	0.193
Cebpb	CCAAT/enhancer binding protein (C/EBP), beta	0.8	0.028	0.4	0.001
Col1a2	Collagen, type I, alpha 2	1.4	0.217	1.2	0.514
Col3a1	Collagen, type III, alpha 1	**2.1**	0.245	1.7	0.472
Ctgf	Connective tissue growth factor	1.0	0.640	0.9	0.006
Cxcr4	Chemokine (C-X-C motif) receptor 4	1.3	0.027	0.9	0.364
Dcn	Decorin	1.0	0.540	1.3	0.001
Edn1	Endothelin 1	1.7	0.120	0.5	0.163
Egf	Epidermal growth factor	**6.5**	0.001	1.1	0.835
Eng	Endoglin	0.9	0.552	0.7	0.034
Faslg	Fas ligand (TNF superfamily, member 6)	0.9	0.196	1.1	0.692
Grem1	Gremlin 1	0.8	0.068	1.2	0.405
Hgf	Hepatocyte growth factor (hepapoietin A; scatter factor)	1.0	0.852	2.2	0.018
Ifng	Interferon, gamma	0.7	0.208	1.4	0.265
Il10	Interleukin 10	0.9	0.220	1.0	0.879
Il13	Interleukin 13	**3.5**	0.001	3.9	0.011
Il13ra2	Interleukin 13 receptor, alpha 2	**7.3**	0.002	6.7	0.004
Il1a	Interleukin 1, alpha	0.6	0.036	0.1	0.001
Il1b	Interleukin 1, beta	0.6	0.004	0.1	0.001
Il4	Interleukin 4	**4.2**	0.001	3.8	0.014
Il5	Interleukin 5	1.5	0.054	1.9	0.002
Ilk	Integrin-linked kinase	0.8	0.051	0.6	0.007
Inhbe	inhibin, beta E	1.0	0.708	0.4	0.435
Itga1	Integrin, alpha 1	1.3	0.001	0.9	0.501
Itga2	Integrin, alpha 2	1.6	0.001	1.8	0.077
Itga3	Integrin, alpha 3	0.7	0.031	0.8	0.479
Itgav	Integrin, alpha V	0.9	0.007	0.9	0.166
Itgb1	Integrin, beta 1	1.1	0.708	0.9	0.632
Itgb3	Integrin, beta 3 (platelet glycoprotein IIIa, antigen CD61)	0.8	0.009	0.6	0.001
Itgb5	Integrin, beta 5	1.0	0.973	1.2	0.328
Itgb6	Integrin, beta 6	0.8	0.291	1.1	0.835
Itgb8	Integrin, beta 8	1.6	0.032	0.5	0.030
Jun	Jun proto-oncogene	0.8	0.537	0.5	0.035
Lox	Lysyl oxidase	1.1	0.311	1.3	0.043
Ltbp1	Latent transforming growth factor beta binding protein 1	0.7	0.126	1.3	0.136
Mmp1	Matrix metallopeptidase 1 (interstitial collagenase)	1.4	0.001	0.9	0.404
Mmp13	Matrix metallopeptidase 13 (collagenase 3)	**4.1**	0.001	1.1	0.835
Mmp14	Matrix metallopeptidase 14 (membrane-inserted)	0.5	0.001	0.2	0.001
Mmp2	Matrix metallopeptidase 2 (gelatinase A)	0.9	0.214	1.1	0.289
Mmp3	Matrix metallopeptidase 3 (stromelysin 1, progelatinase)	0.9	0.344	0.6	0.014
Mmp8	Matrix metallopeptidase 8 (neutrophil collagenase)	1.1	0.794	1.1	0.759
Mmp9	Matrix metallopeptidase 9 (gelatinase B)	0.8	0.005	1.3	0.004
Myc	V-myc myelocytomatosis viral oncogene homolog (avian)	1.1	0.001	1.0	0.476
Nfkb1	Nuclear factor of kappa light polypeptide gene enhancer in B-cells 1	0.6	0.001	0.3	0.001
Pdgfa	Platelet-derived growth factor alpha polypeptide	0.8	0.204	1.2	0.373
Pdgfb	Platelet-derived growth factor beta polypeptide	0.6	0.001	0.8	0.004
Plat	Plasminogen activator, tissue	0.5	0.001	0.5	0.001
Plau	Plasminogen activator, urokinase	1.0	0.724	0.4	0.001
Plg	Plasminogen	0.8	0.291	1.1	0.835

Serpina1	Serpin peptidase inhibitor, clade A, member 1	1.0	0.505	0.6	0.001
Serpine1	Serpin peptidase inhibitor, clade E, member 1	0.9	0.531	0.7	0.089
Serpinh1	Serpin peptidase inhibitor, clade H (heat shock protein 47), member 1	1.0	0.357	1.3	0.004
Smad2	SMAD family member 2	0.9	0.399	0.8	0.214
Smad3	SMAD family member 3	**0.4**	0.019	0.2	0.005
Smad4	SMAD family member 4	1.1	0.647	0.9	0.435
Smad6	SMAD family member 6	0.6	0.022	0.6	0.005
Smad7	SMAD family member 7	1.0	0.972	0.6	0.432
Snai1	Snail homolog 1 (Drosophila)	1.3	0.307	0.7	0.336
Sp1	Sp1 transcription factor	1.1	0.319	0.9	0.707
Stat1	Signal transducer and activator of transcription 1, 91kDa	1.3	0.005	2.9	0.001
Stat6	Signal transducer and activator of transcription 6, interleukin-4 induced	1.2	0.270	1.0	0.899
Tgfb1	Transforming growth factor, beta 1	0.8	0.036	0.6	0.034
Tgfb2	Transforming growth factor, beta 2	1.0	0.914	0.6	0.002
Tgfb3	Transforming growth factor, beta 3	0.9	0.314	0.8	0.091
Tgfbr1	Transforming growth factor, beta receptor 1	0.9	0.753	0.7	0.008
Tgfbr2	Transforming growth factor, beta receptor II (70/80kDa)	1.2	0.587	0.9	0.523
Tgif1	TGFB-induced factor homeobox 1	1.4	0.258	1.3	0.356
Thbs1	Thrombospondin 1	1.0	0.940	0.2	0.004
Thbs2	Thrombospondin 2	0.9	0.170	0.7	0.004
Timp1	TIMP metallopeptidase inhibitor 1	1.0	0.835	0.7	0.037
Timp2	TIMP metallopeptidase inhibitor 2	1.5	0.040	1.5	0.103
Timp3	TIMP metallopeptidase inhibitor 3	0.8	0.023	2.3	0.001
Timp4	TIMP metallopeptidase inhibitor 4	0.5	0.007	1.3	0.042
Tnf	Tumor necrosis factor	0.8	0.030	0.3	0.001
Vegfa	Vascular endothelial growth factor A	1.2	0.088	0.5	0.003

*****Statistically significant (*P*<0.05) and biologically relevant (≤ 0.5, bold gold or ≥ 2, bold red) PDE #1-induced fold changes are analysed in Results, Table 2

******Compared to Control group.

Table 3. Changes in fibrosis-related peritoneal gene expression (complete fibrosis array) at day 28 in mice infected with *S. epidermidis* or *S. epidermidis* + sTLR2.*****

		S. epidermidis		***S. epidermidis* + sTLR2**	
Gene symbol	**Description**	**Fold Change****	***P*-value****	**Fold Change****	***P*-value****
Acta2	Actin, alpha 2, smooth muscle, aorta	1.1	0.133	1.1	0.339
Agt	Angiotensinogen (serpin peptidase inhibitor, clade A, member 8)	1.1	0.304	0.8	0.390
Akt1	Thymoma viral proto-oncogene 1	1.7	0.048	1.3	0.315
Bcl2	B-cell leukemia/lymphoma 2	1.5	0.167	1.3	0.333
Bmp7	Bone morphogenetic protein 7	1.9	0.029	1.7	0.068
Cav1	Caveolin 1, caveolae protein	1.5	0.062	1.2	0.283
Ccl11	Chemokine (C-C motif) ligand 11	1.0	0.772	1.0	0.992
Ccl12	Chemokine (C-C motif) ligand 12	**12.4**	0.008	9.4	0.023
Ccl3	Chemokine (C-C motif) ligand 3, MIP1a	**4.3**	0.033	5.2	0.005
Ccr2	Chemokine (C-C motif) receptor 2	**4.2**	0.043	2.5	0.082
Cebpb	CCAAT/enhancer binding protein (C/EBP), beta	1.8	0.001	1.4	0.099
Col1a2	Collagen, type I, alpha 2	1.1	0.625	0.7	0.105
Col3a1	Collagen, type III, alpha 1	1.1	0.507	0.9	0.760
Ctgf	Connective tissue growth factor	1.6	0.138	3.2	0.034
Cxcr4	Chemokine (C-X-C motif) receptor 4	**2.1**	0.036	1.7	0.113
Dcn	Decorin	1.1	0.593	1.1	0.669
Edn1	Endothelin 1	0.8	0.078	1.0	0.972
Egf	Epidermal growth factor	1.8	0.004	1.3	0.103
Eng	Endoglin	1.7	0.001	1.	0.080
Fasl	Fas ligand (TNF superfamily, member 6)	**8.0**	0.048	3.2	0.209
Grem1	Gremlin 1	1.2	0.527	0.8	0.283
Hgf	Hepatocyte growth factor	**9.8**	0.048	3.7	0.050
Ifng	Interferon gamma	**14.1**	0.018	15.3	0.004
Il10	Interleukin 10	**8.7**	0.010	2.5	0.001
Il13	Interleukin 13	0.7	0.152	1.0	0.688
Il13ra2	Interleukin 13 receptor, alpha 2	0.9	0.765	1.0	0.841
Il1a	Interleukin 1 alpha	1.0	0.714	0.4	0.091
Il1b	Interleukin 1 beta	**7.8**	0.046	5.5	*0.049*
Il4	Interleukin 4	0.9	0.677	1.1	0.515
Il5	Interleukin 5	2.3	0.234	2.7	0.251
Il6	Interleukin 6	**3.1**	0.001	1.4	0.218
Ilk	Integrin linked kinase	1.2	0.324	1.1	0.549
Inhbe	Inhibin beta E	1.2	0.530	1.1	0.841
Itga1	Integrin alpha 1	1.8	0.002	1.5	0.057
Itga2	Integrin alpha 2	**5.4**	0.019	3.6	0.076
Itga3	Integrin alpha 3	1.0	0.909	0.8	0.137
Itgav	Integrin alpha V	1.5	0.100	1.1	0.562
Itgb1	Integrin beta 1 (fibronectin receptor beta)	1.9	0.019	1.4	0.120
Itgb3	Integrin beta 3	**2.2**	0.000	1.6	0.000
Itgb5	Integrin beta 5	1.6	0.000	1.3	0.024
Itgb6	Integrin beta 6	1.2	0.138	0.9	0.245
Itgb8	Integrin beta 8	3.1	0.080	2.7	0.125
Jun	Jun oncogene	1.6	0.016	1.6	0.023
Lox	Lysyl oxidase	1.0	0.817	1.1	0.564
Ltbp1	Latent transforming growth factor beta binding protein 1	1.9	0.103	1.7	0.077
Mmp13	Matrix metallopeptidase 13	**4.4**	0.037	1.5	0.344
Mmp14	Matrix metallopeptidase 14 (membrane-inserted)	1.8	0.242	1.0	0.998
Mmp1a	Matrix metallopeptidase 1a (interstitial collagenase)	1.2	0.253	1.1	0.283
Mmp2	Matrix metallopeptidase 2	1.3	0.362	1.3	0.152
Mmp3	Matrix metallopeptidase 3	0.8	0.263	0.5	0.014
Mmp8	Matrix metallopeptidase 8	1.7	0.215	1.9	0.070
Mmp9	Matrix metallopeptidase 9	1.3	0.017	0.4	0.009
Myc	Myelocytomatosis oncogene	**2.1**	0.005	1.7	0.078
Nfkb1	Nuclear factor of kappa light polypeptide gene enhancer in B-cells 1	1.5	0.049	1.1	0.230
Pdgfa	Platelet derived growth factor, alpha	1.1	0.679	1.0	0.748
Pdgfb	Platelet derived growth factor, B polypeptide	1.6	0.060	1.3	0.001

Plat	Plasminogen activator, tissue	0.9	0.482	0.7	0.024
Plau	Plasminogen activator, urokinase	1.4	0.227	1.0	0.698
Plg	Plasminogen	0.9	0.765	1.6	0.411
Serpina1a	Serine (or cysteine) peptidase inhibitor, clade A, member 1a	0.9	0.765	1.1	0.841
Serpine1	Serine (or cysteine) peptidase inhibitor, clade E, member 1	**3.5**	0.022	2.1	0.002
Serpinh1	Serine (or cysteine) peptidase inhibitor, clade H, member 1	1.3	0.051	1.0	0.874
Smad2	MAD homolog 2 (Drosophila)	**2.0**	0.018	1.4	0.037
Smad3	MAD homolog 3 (Drosophila)	1.6	0.014	1.4	0.192
Smad4	MAD homolog 4 (Drosophila)	1.4	0.126	1.2	0.355
Smad6	MAD homolog 6 (Drosophila)	1.4	0.048	1.1	0.598
Smad7	MAD homolog 7 (Drosophila)	1.7	0.099	1.5	0.178
Snai1	Snail homolog 1 (Drosophila)	1.7	0.120	1.0	0.864
Sp1	Trans-acting transcription factor 1	**2.2**	0.002	1.5	0.046
Stat1	Signal transducer and activator of transcription 1	**8.1**	0.046	6.4	*0.041*
Stat6	Signal transducer and activator of transcription 6	1.6	0.010	1.2	0.107
Tgfb1	Transforming growth factor, beta 1	1.9	0.170	1.2	0.042
Tgfb2	Transforming growth factor, beta 2	1.5	0.050	1.0	0.963
Tgfb3	Transforming growth factor, beta 3	1.2	0.299	1.2	0.002
Tgfbr1	Transforming growth factor, beta receptor I	**2.4**	0.001	1.6	0.101
Tgfbr2	Transforming growth factor, beta receptor II	1.6	0.021	0.9	0.708
Tgif1	TGFB-induced factor homeobox 1	1.5	0.575	1.1	0.793
Thbs1	Thrombospondin 1	2.6	0.139	2.2	0.019
Thbs2	Thrombospondin 2	1.1	0.477	0.9	0.856
Timp1	Tissue inhibitor of metalloproteinase 1	**3.2**	0.028	1.5	0.233
Timp2	Tissue inhibitor of metalloproteinase 2	1.1	0.528	0.8	0.383
Timp3	Tissue inhibitor of metalloproteinase 3	1.6	0.006	1.6	0.033
Timp4	Tissue inhibitor of metalloproteinase 4	0.8	0.834	1.5	0.086
Tnf	Tumor necrosis factor	**8.1**	0.042	14.3	0.043
Vegfa	Vascular endothelial growth factor A	1.2	0.313	0.9	0.420

*****Statistically significant (P<0.05) and biologically relevant (≤ 0.5 or ≥ 2) *S. epidermidis*-induced fold changes in bold red are analysed in Results, Table 3

******Compared to Control group.